Synthesis and Redox Behavior of Ruthenocene-Terminated Oligoenes: Characteristic and Stable Two-Electron Redox System and Lower Potential Shift of the Two-Electron Oxidation Wave with Elongating Conjugation

Masaru Sato,*[a] Toru Nagata,[a] Atsushi Tanemura,[a] Takashi Fujihara,[a] Shigekazu Kumakura,[a] and Kei Unoura[b]

Abstract: Ruthenocene-terminated butadienes and hexatrienes were prepared by the Wittig reaction of 3-ruthenocenyl-2-propenals with ruthenocenylmethylphosphonium salts and the Mukaiyama coupling of the propenals, respectively. Cyclic voltammetry of these complexes indicated that they were involved in a stable two-electron redox process. The oxidation potentials for ruthenocene-terminated oligoenes shifted progressively to lower potential with the increasing CH=CH units as follows: Rc–Rc (0.32 V) > RcCH=CHRc (+0.09 V) > Rc(CH=CH)$_2$Rc (−0.06 V) > Rc(CH=CH)$_3$Rc (−0.07 V), (Rc = ruthenocene). The tendency is in remarkable contrast to that in the successive one-electron redox process. These complexes were chemically oxidized to give stable crystalline solids, whose structures were confirmed by NMR spectroscopy and X-ray analysis to be oligoene analogues of a bis(fulvene) complex, for example, [(η^5-C_5Me_5)Ru{μ_2-η^6:η^6-C_5H_4CH(CH=CH)$_n$-CHC_5H_4}Ru(η^5-C_5Me_5)]$^{2+}$ (n = 1 or 2). The DFT calculation of the two-electron-oxidized species reproduced well the fulvene-complex structure for the ruthenocene moieties. Since both the neutral and oxidized species are stable and chemically reversible, this redox system may be serviceable as a two-electron version of the ferrocene one-electron redox system.

Keywords: alkene ligands · oxidation · redox chemistry · ruthenium · ruthenocene

Introduction

Binuclear organometallic complexes can be regarded as organometallic versions of the multistage redox systems first reviewed by Deuchert and Hönig.[1] They undergo one- or two-electron oxidation to afford the one- or two-electron-oxidized species that can be stabilized by the electron delocalization, depending on the character of the metals and the bridging ligands (Scheme 1). A large number of dinuclear complexes with π-conjugated bridges have been reported from the attraction in both fundamental and applied studies.[2,3] Of them, the chemistry of bis(ferrocenyl) derivates has been well investigated, especially from the viewpoint of mixed-valence complexes, because ferrocene has a well-defined and stable one-electron redox system.[4,5] In the search for building blocks for molecular wires (electronic communication)[6] and other technological potential applications, much interest has been recently focused on oligoyne derivatives with the organometallic end groups.[7] In the complexes, [Cp*(NO)(Ph_3P)Re(C≡C)$_n$Re(PPh_3)(NO)Cp*][8] and [Cp*(dppe)Fe(C≡C)$_n$Fe(dppe)Cp*],[9] two successive one-electron redox processes were confirmed and both oxidized species were characterized. The structure of the two-electron-oxidized species, which involved a rearrangement of

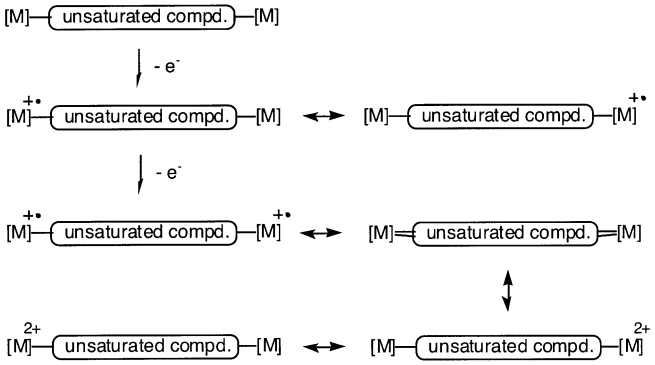

Scheme 1.

[a] Prof. M. Sato, T. Nagata, A. Tanemura, Prof. T. Fujihara, Prof. S. Kumakura
Department of Chemistry, Faculty of Science
Saitama University, Saitama, Saitama 338-8570 (Japan)
Fax: (81) 48-858-3700
E-mail: msato@chem.saitama-u.ac.jp

[b] Prof. K. Unoura
Department of Chemistry, Faculty of Science
Yamagata University, Kosirogawa, Yamagata 990-8560 (Japan)

DOI: 10.1002/chem.200306004

the multiple bond, was determined by a X-ray diffraction. A similar two-step redox behavior was observed in the diene-bridged complexes, $[CpFeL_2(CH{=}CH)_2FeL_2Cp]$,[10] and the triene-bridged complexes, $[X(CO)(Ph_3P)_2Ru(CH{=}CH)_3Ru(PPh_3)_2(CO)X]$.[11] The redox properties of the ferrocene-terminated oligoenes was fully investigated.[12] Additionally, a four-step redox process was found in the Ru-caped diyne complexes.[13] In organobimetallic complexes, on the other hand, a few two-electron redox systems have been found in which the one-electron oxidized species is not detected and an interesting structural rearrangement of the ligands is incidental to the redox process.[14–17] We have previously reported the two-electron oxidation of diruthenocene,[18] 1,2-bis(ruthenocenyl)ethenes,[19] and 1,2-bis(ruthenocenyl)ethynes,[20] in which a remarkable structural rearrangement was observed. Among these systems, especially, both bis(ruthenocenyl)ethenes and the two-electron-oxidized species were stable in air and the two-electron redox system was chemically reversible. Therefore, the effect of elongated bridging π-conjugation to the electrochemistry and the properties is a question of great interest. Such effects were also investigated in the successive one-electron redox systems, $[Cp^*(NO)(Ph_3P)Re(C{\equiv}C)_nRe(PPh_3)(NO)Cp^*]$,[8e,f] $[Cp^*(dppe)Fe(C{\equiv}C)_nFe(dppe)Cp^*]$,[9c,f] and $[Fc(CH{=}CH)_nFc]$ (Fc = ferrocenyl).[12a] We now report the synthesis, redox behavior, and chemical oxidation of ruthenocene-terminated oligoenes.

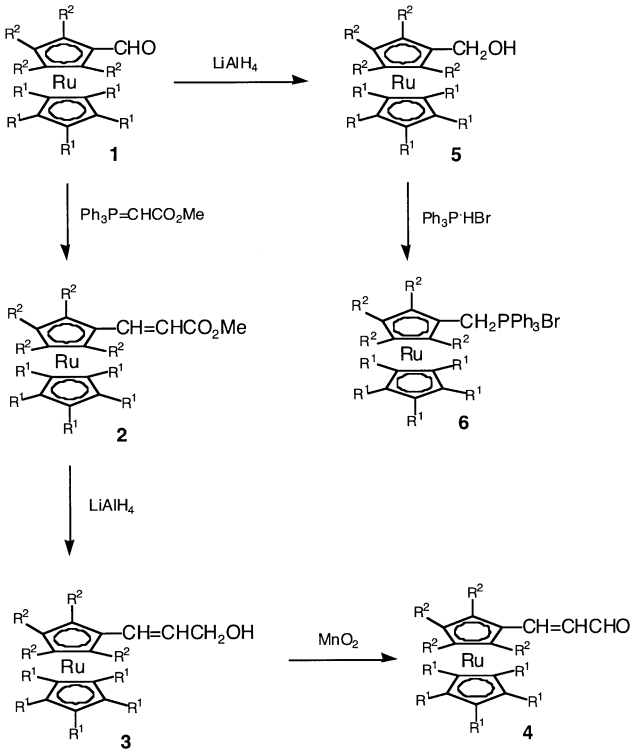

Scheme 2. **a**: $R^1 = R^2 = H$; **b**: $R^1 = Me$, $R^2 = H$; **c**: $R^1 = H$, $R^2 = Me$.

Results and Discussion

Syntheses. The synthesis of bis(ruthenocenyl)ethenes, [RcCH=CHRc], [Rc*CH=CHRc*], and [Rc′CH=CHRc′] (Rc = ruthenocenyl, Rc* = 1′,2′,3′,4′,5′-pentamethylruthenocenyl, and Rc′ = 2,3,4,5-tetramethylruthenocenyl) has been reported previously.[19,21] The preparation of 1,4-bis(ruthenocenyl)butadienes, $[Rc(CH{=}CH)_2Rc]$, $[Rc^*(CH{=}CH)_2Rc^*]$, and $[Rc'(CH{=}CH)_2Rc']$, was carried out by the Wittig reaction of 3-ruthenocenyl-1-propenals and ruthenocenylmethyl(triphenyl)phosphonium bromides, which were prepared according to the processes shown in Scheme 2. Ruthenocenylcarbaldehyde (**1a**) was treated with carbomethoxymethyl(triphenyl)phosphorane in CH_2Cl_2 to give methyl 3-ruthenocenylacrylate (**2a**) as a mixture of *E* and *Z* isomers in 90 and 5% yields, respectively. In a similar procedure, 1′,2′,3′,4′,5′-pentamethylruthenocenylcarbaldehyde (**1b**) and 2,3,4,5-tetramethylruthenocenycarbaldehyde (**1c**) afforded methyl 3-(1″,2″,3″,4″,5″-pentamethylruthenocenyl)acrylate (**2b**) and methyl 3-(2′,3′,4′,5′-tetramethylruthenocenyl)acrylate (**2c**) , respectively, in good yields. After the separation of the *E* isomers by chromatography on silica gel, the separated isomers of the esters **2a**–**2c** were reduced with $LiAlH_4$ or $LiAlH_4/AlCl_3$ in THF to give the corresponding unsaturated alcohols **3a**–**3c**, respectively, in excellent yields. The propenols **3a**–**3c** were oxidized with MnO_2 in refluxing dichloroethane to give the corresponding propenals **4a**–**4c**, respectively, in good yields. On the other hand, the reduction of the aldehydes **1a**–**1c** with $LiAlH_4$ led to the corresponding alcohols **5a**–**5c**, respectively, in excellent yields, which were then treated with triphenylphoshine hydrobromide in refluxing toluene to give the corresponding phosphonium salts **6a**–**6c**, respectively, in quantitative yields.

The propenal **4a** was treated with the ylide solution prepared from the reaction of the phosphonium bromide **6a** with LDA at low temperature to afford a mixture of *E*,*E* and *E*,*Z* isomers (5:4) of 1,4-bis(ruthenocenyl)butadiene, $[Rc(CH{=}CH)_2Rc]$ (**7a**), in 78% yield. In a similar procedure, 1,4-bis(1″,2″,3″,4″,5″-pentamethylruthenocenyl)butadiene, $[Rc^*(CH{=}CH)_2Rc^*]$ (**7b**), and 1,4-bis-(2′,3′,4′,5′-tetramethylruthenocenyl)butadiene, $[Rc'(CH{=}CH)_2Rc']$ (**7c**), were obtained as mixtures (3:2 and 13:1) of *E*,*E* and *E*,*Z* isomers in 46 and 59% yields, respectively (Scheme 3). Almost pure *E*,*E* isomers of **7a**–**7c** were isolated by the repeated fractional recrystallization from benzene. Their stereochemistry was assigned by their ^1H NMR spectra. For example, the ^1H NMR spectrum of complex (*E*,*E*)-**7b** in C_6D_6 showed the olefinic protons as an AA′XX′ pattern at $\delta = 5.93$ ($H_{1,4}$) and 6.25 ppm ($H_{2,3}$) ($J_{1,2} = J_{3,4} = 15.3$ and $J_{2,3} = 10.6$ Hz). The structure of (*E*,*E*)-**7a** was determined by X-ray diffraction. The ORTEP view of (*E*,*E*)-**7a** is shown in Figure 1; selected bond lengths and angles are given in the figure legend. Two ruthenocenyl groups are positioned on the opposite side of the mean plane of the bridging diene. Both double bonds in the bridging diene adopt an *E* configuration and are connected to each other in an s-*trans* conformation. The plane of the diene is nearly coplanar (4.8°) with the substituted cyclopentadienyl (Cp) ring of the ruthenocene nucleus. The C(1)–C(1) (1.447(6) Å) and C(1)–C(2) (1.363(6) Å) bond lengths are normal for single and double bonds, respectively, of a conjugated diene.

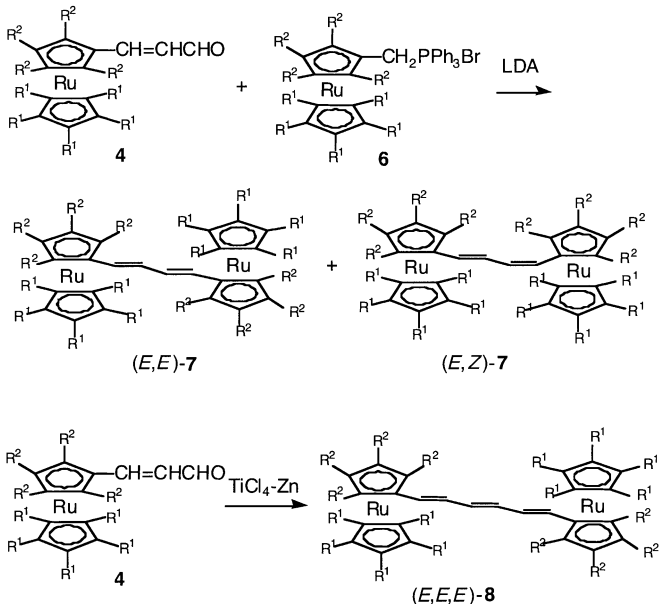

Scheme 3. **a**: $R^1=R^2=H$; **b**: $R^1=Me$, $R^2=H$; **c**: $R^1=H$, $R^2=Me$.

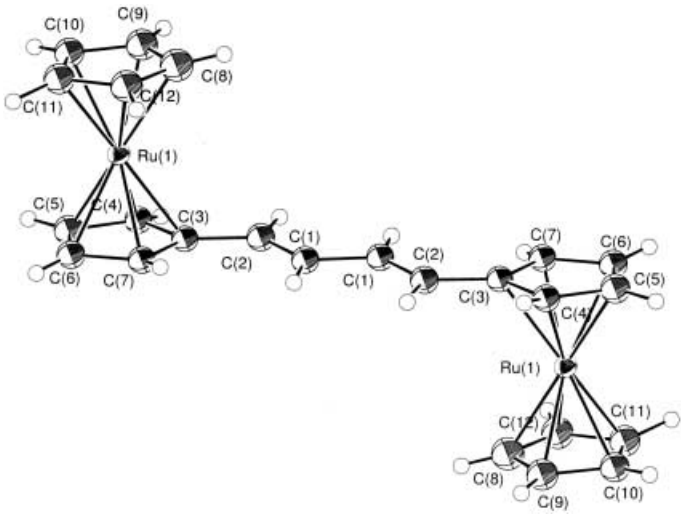

Figure 1. ORTEP view of (*E*,*E*)-**7a**. Selected bond lengths [Å] and angles [°]: C(1)–C(1) = 1.447(6), C(1)–C(2) = 1.363(6), C(2)–C(3) = 1.457(6), Ru(1)–C(Cp) = 2.188(av), C(Cp)–C(Cp) = 1.429(av), C(1)-C(1)-C(2) = 122.3 (4), C(1)-C(2)-C(3) = 125.0(4), C(2)-C(3)-C(4) = 124.1(4).

The propenal derivative **4a** was allowed to react with a low-valent Ti reagent prepared from $TiCl_4$ and Zn powder in THF at low temperature, followed by refluxing, to give 1,6-bis(ruthenocenyl)hexatriene, [Rc(CH=CH)$_3$Rc] (**8a**), in 29% yield as a single isomer (Scheme 3). In a similar manner, 1,6-bis(1″,2″,3″,4″,5″-pentamethylruthenocenyl)hexatriene, [Rc*(CH=CH)$_3$Rc*] (**8b**), and 1,6-bis-(2′,3′,4′,5′-tetramethylruthenocenyl)hexatriene, [Rc′(CH=CH)$_3$Rc′] (**8c**), were obtained from **4b** and **4c**, respectively, in moderate yields. In the ^{1}H NMR spectrum of **8b** in C_6D_6, the olefinic protons appeared as an AA′BB′XX′ pattern at $\delta = 6.42$ ($H_{2,5}$), 6.35 ($H_{3,4}$), and 6.05 ppm ($H_{1,6}$). The simulation of the olefinic proton signals afforded the following coupling constants: $J_{1,2}=J_{3,4}=J_{5,6}=15.8$ Hz and $J_{2,3}=J_{4,5}=10.6$ Hz. The ^{13}C NMR spectrum of **8b** showed three olefinic carbons at $\delta = 125.85$, 128.15, and 130.87 ppm. These NMR data are consistent with the triene derivatives with an *E*,*E*,*E* configuration.

The UV-visible spectral data of **7a**–**7c** and **8a**–**8c** measured in CH_2Cl_2 are collected in Table 1, along with those of the ethene derivatives. The spectra of **7b**, **8b**, and [Rc*CH=CHRc*] are shown in Figure 2, for example. The two absorption bands observed, which might be assigned to the π–π* transition on the basis of the strength of the absorption, were shifted to longer wavelength region and increased their absorbance with the elongation of the conjugation, as

Table 1. The UV-visible spectroscopic data of compounds **7a**–**7c**, **8a**–**8c**, and related compounds in CH_2Cl_2.

Compound	λ_{max} [nm](ε)	
[RcCH=CHRc]	287(16200)	331 sh(4700)
7a	309(30200)	350 sh(14800)
8a	331(30200)	376(26700)
[Rc*CH=CHRc*]	295(22100)	337 sh(9800)
7b	320(26300)	371(21200)
8b	342(28100)	395(33700)
[Rc′CH=CHRc′]	283(17300)	331 sh(4300)
7c	311(32000)	356 sh(16100)
8c	335(33700)	374(29800)

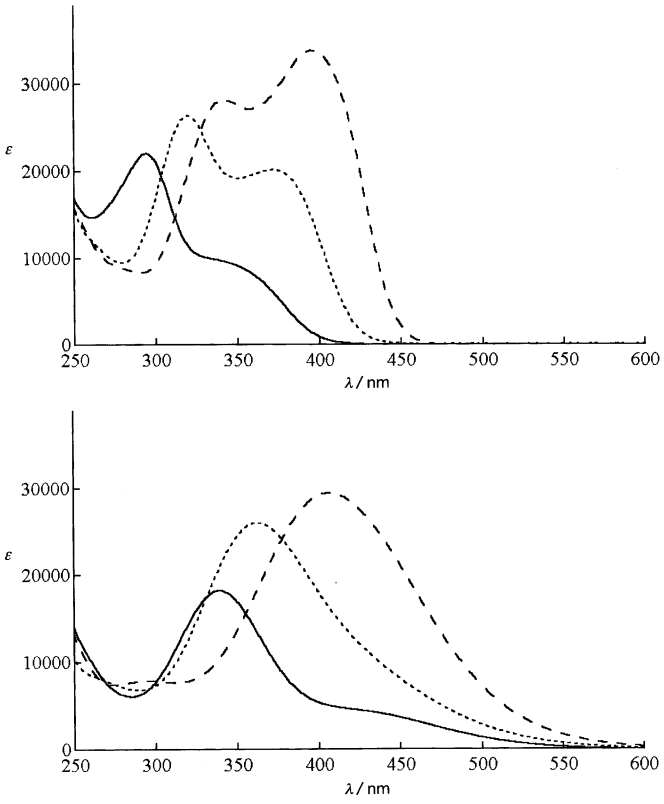

Figure 2. Electronic spectra for the neutral complexes (top), [Rc*CH=CHRc*] (——), **7b** (– – –), and **8b** (•••••) and for the oxidized species (bottom) of [Rc*CH=CHRc*] (——), **7b** (**9b**) (– – –), and **8b** (**10b**) (•••••).

expected. The wavelength-shift caused by the increase of one double bond ($\Delta\lambda = 18$–34 nm) in the ruthenocenyl series is similar to that found in the ferrocenyl series ($\Delta\lambda = 16$–37 nm).[12a] The absorbance of the longer wavelength absorption increased to a greater extent with the extending conjugation, relative to that of the shorter wavelength absorption.

Redox behavior: The cyclic voltammograms of **7a**–**7c** and **8a**–**8c** and related complexes were measured in CH_2Cl_2 and the electrochemical data are summarized in Table 2. The voltammograms for [Rc*CH=CHRc*], **7b**, and **8b** are exhibited in Figure 3, as an example. As seen clearly from Table 2 and Figure 3, the electron transfer in every wave was not reversible ($\Delta E = E_{pc} - E_{pa} = 0.09$–$0.16$ V); however, the oxidation wave was accompanied by a reduction wave with nearly the same magnitude as that of the oxidation wave ($i_{pa}/i_{pc} = 0.83$–1.01), except in the case of [RcCH=CHRc] and [Rc′CH=CHRc′]. These last two complexes showed two reduction waves that may suggest some instability in the two-electron-oxidized species. In the complexes cited in Table 2, only the one redox process was observed within the potential window of CH_2Cl_2 and no other wave appeared above 0.7 V, while ruthenocene itself showed only the irreversible two-electron oxidation wave at 0.53 V under usual conditions.[22] Only in the CV of Rc–Rc, a small second oxidative process was observed at approximately 0.7 V and a complex re-reductive process appeared on the turn of the scan at 1.0 V. As shown in Table 2, the electron count (n) obtained from the thin-layer coulometry is nearly 2.0 for any complex, proving that the observed waves correspond to a two-electron redox process. The nonreversible features in the CV of the ruthenocene-terminated oligoenes described above may suggest that the oxidation and reduction peaks represent an electron-transfer reaction followed by a chemical reaction (vide infra). As seen in Table 2, the oxidation waves of **7a**–**7c** and **8a** - **8c** were observed in considerably lower potential region (ΔE_{pa} = ca. 0.3–0.5 V) than those of the corresponding mononuclear ruthenocene derivatives, similar to that in ethene derivatives.[19] Moreover, their oxidation potentials shifted to lower potential region with the increase of the bridging double bond as follows: [Rc–Rc] (+0.32 V)[18] > [RcCH=CHRc] (+0.09 V)[19] > [Rc(CH=CH)$_2$Rc] (**7a**) (−0.06 V) > [Rc(CH=CH)$_3$Rc] (**8a**) (−0.07 V), for example. A similar tendency was also observed in the Rc* and Rc′ series, as seen in Table 2. The tendency is in sharp contrast to that in the successive one-electron redox system found previously. In diferrocenylpolyenes, [Fc(CH=CH)$_n$Fc],[13a] for example, the first redox potentials are observed at lower potential than that of ferrocene itself although the second redox potentials remain intact in the shorter ethene bridge ($n = 1$–3), but the first redox potentials gradually ascend with the increasing double bonds and then a single redox potential is observed for $n = 4$–6. A similar tendency was also observed in the ethyne-bridged binuclear complexes, [Cp*(NO)(Ph$_3$P)Re(C≡C)$_n$Re(PPh$_3$)(NO)Cp*][9e,f] and [Cp*(dppe)Fe(C≡C)$_n$Fe(dppe)Cp*].[10c,f] In our bis(ruthenocenyl)oligoene systems, the two-electron oxidation potentials are shifted to lower potential region with elongation of the oligoene bridge, as shown in above. Moreover, the potentials that converge with the increasing conjugation (e.g., ca. −0.10 V for the Rc series) are considerably lower than that of ruthenocene itself (0.53 V). This suggests that the two-electron-oxidized species of bis(ruthenocenyl)oligoenes are largely stabilized by certain factors related to the structural isomerization and so forth.

Table 2. Electrochemical data for the complexes in CH_2Cl_2.[a]

	E_{pa} [V^{-1}]	E_{pc} [V^{-1}]	ΔE/	Vi_{pa}/i_{pc}	n[b]
[Rc–Rc]	0.32	0.16	0.16	0.87	1.9
[RcCH=CHRc]	0.09	−0.06	0.15	irrev.	–[c]
7a	−0.06	−0.16	0.10	0.88	2.0
8a	−0.07	−0.16	0.09	0.85	2.0
[Rc*CH=CHRc*]	−0.20	−0.31	0.11	1.01	1.8
7b	−0.19	−0.31	0.13	0.83	2.0
8b	−0.27	−0.37	0.10	0.96	1.9
[Rc′CH=CHRc′]	−0.08	−0.16	0.09	0.51	2.0
7c	−0.23	−0.33	0.10	0.98	2.1
8c	−0.22	−0.35	0.13	0.96	1.9

[a] Sweep rate = 0.1 V s^{-1}, V vs FcH/FcH$^+$. [b] Determined by thin-layer coulometry. [c] Not measured because of the slow dissolution and the shoulder accompanied.

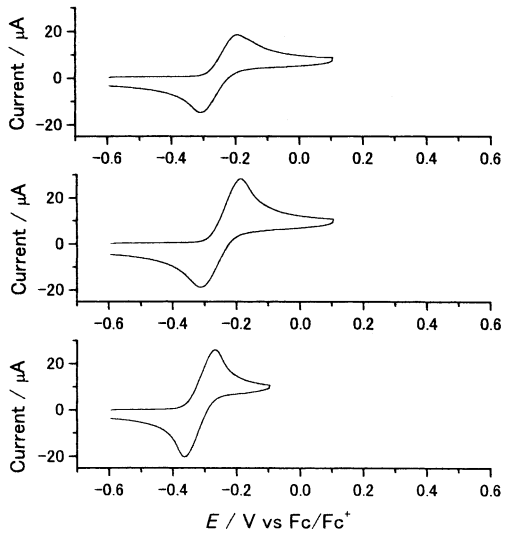

Figure 3. Cyclic votammograms for [Rc*CH=CHRc*] (top), **7b** (middle), and **8b** (bottom) in CH_2Cl_2 (sweep rate = 0.1 V s^{-1}, [complex] = 0.5–0.6 mmol).

Chemical oxidation: The two-electron oxidation of bis(ruthenocenyl)ethenes afforded the stable dicationic complexes.[19] Similarly, complexes **7a**–**7c** and **8a**–**8c** were oxidized with two equivalents of *p*-BQ/BF_3·OEt_2 (BQ = benzo-

quinone) at 0 °C in CH_2Cl_2 to give the corresponding dicationic complexes **9a**–**9c** and **10a**–**10c**, respectively, as stable solids in high yields (Scheme 4). The oxidized complexes were soluble in CD_3CN, CD_3NO_2, and $(CD_3)_2CO$. Solutions of **9a**–**9c** in CD_3CN and CD_3NO_2 were stable at room temperature for a long time, but **10a**–**10c** were somewhat unstable in the same solvents and changed color after a few days. Electronic spectral data of the oxidized complexes, **9a**–**9c**, **10a**, and **10b**, are collected in Table 3, along with those of related complexes. The spectra of **9b**, **10b**, and the oxidized [Rc*CH=CHRc*] are shown in Figure 2, as an example. The absorption bands observed with large absorbance, probably due to the CT-transition, shifted to the longer wavelength region with the extension of the conjugation. The extent of the shift per one double bond ($\Delta\lambda = 23$–52 nm) is somewhat larger than that in the corresponding neutral complexes.

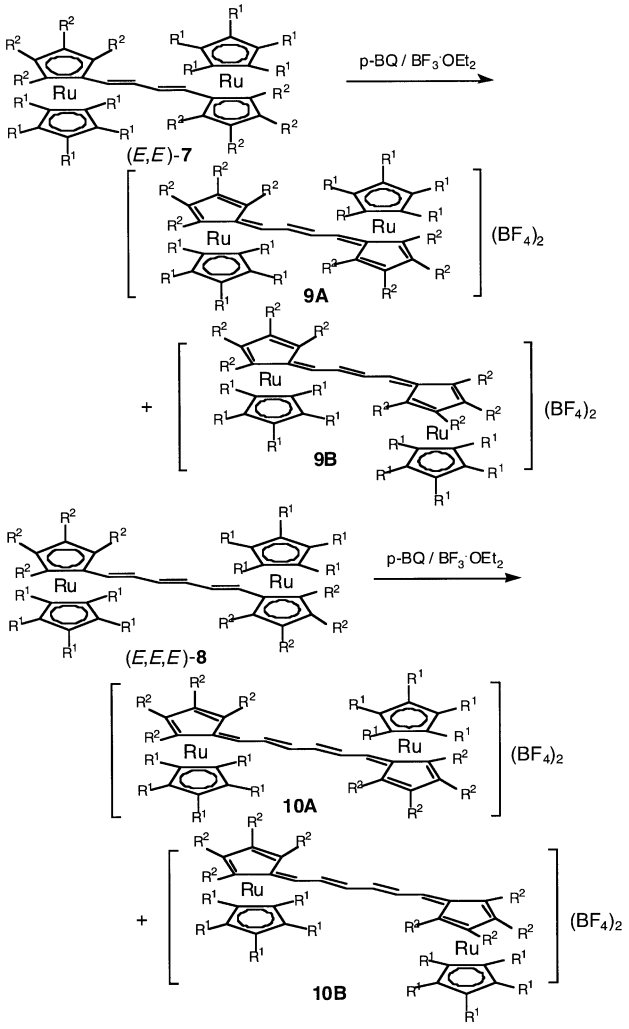

Scheme 4. **a**: $R^1 = R^2 = H$; **b**: $R^1 = Me$, $R^2 = H$; **c**: $R^1 = H$, $R^2 = Me$.

Table 3. The UV-visible spectroscopic data of compounds **9a**–**9c** **10a**, **10b**, and related comounds in CH_3CN.

Compound	λ_{max} [nm](ε)	
$[RcCH=CHRc]^{2+}$	292(10500)	383(2600)
9a	335(21500)	
10a	387(29600)	
$[Rc*CH=CHRc*]^{2+}$	339(18200)	420sh(4500)
9b	362(26000)	
10b	407(29400)	
$[Rc'CH=CHRc']^{2+}$	292(13000)	382sh(2900)
9c	334(21100)	

The ^1H NMR spectrum of **9b** in CD_3NO_2 showed one Me proton signal at $\delta = 1.97$ ppm and one set of olefinic proton signals at $\delta = 6.07$ and 6.63 ppm, indicating that the oxidized species adopted a structure with a symmetrical face or a center of symmetry. The proton signals of the C_5H_4 rings of **9b** appeared as broad doublets at $\delta = 4.97$ and 5.51 ppm and as a triplet of doublets at δ05.85 and 5.94 ppm ($J = 2.9$ and 1.1 Hz), indicating that the C_5H_4-ring protons were in an unsymmetrical environment, in contrast to those in the corresponding neutral complex **7b**. From the H,H-COSY spectrum of **9b**, the signal sets in the higher ($\delta = 4.97$ and 5.51 ppm) and the lower fields ($\delta = 5.85$ and 5.94 ppm) were assigned to the α- and β-protons of the C_5H_4-ring, respectively, because a strong correlation was recognized between the latter signals, but only a weak correlation between the former signals. They were also observed in a considerably lower field relative to the corresponding signals in **7b** ($\Delta\delta =$ 0.67–1.57 ppm), indicating the accumulation of the positive charge on the Ru atoms. These features observed in **9b** are similar to those observed in the ethene-bridged analogues, $[Ru_2(\mu_2\text{-}\eta^6\text{:}\eta^6\text{-}C_5H_4CHCHC_5H_4)(\eta\text{-}C_5Me_5)_2]^{2+}$, in which the C_5H_4-ring protons were observed at $\delta = 4.93$, 5.43, 5.86, and 5.98 ppm.[19] In the ^{13}C NMR spectrum of **9b**, the signals of the C_5H_4-ring carbon atoms were observed as two sets of signals largely separated (at $\delta = 80.81$ and 83.58 ppm for the α-carbon signals and at $\delta = 96.92$ and 97.29 ppm for the β-carbon signals) at lower field than those in **7b**. (cf. $\delta = 81.59$ and 84.10 ppm for the α-carbon signals and $\delta = 97.32$ and 99.15 ppm for the β-carbon signals in $[Ru_2(\mu_2\text{-}\eta^6\text{:}\eta^6\text{-}C_5H_4CHCHC_5H_4)(\eta\text{-}C_5Me_5)_2]^{2+}$).[19] The signal for both terminal carbon atoms in the bridging butadiene in **9b** appeared at $\delta = 100.13$ ppm, the chemical shift of which was shifted considerably to higher field than that of the corresponding carbon signal in **7b** ($\delta = 126.18$ ppm), suggesting the coordination of the carbon atom to the Ru metal. These ^1H and ^{13}C NMR spectral data confirm that the $(\eta\text{-}C_5Me_5)\text{-}Ru(C_5H_4CH)$ moiety in **9b** adopts a fulvene-complex structure, similar to that in $[Ru_2(\mu_2\text{-}\eta^6\text{:}\eta^6\text{-}C_5H_4CHCHC_5H_4)(\eta\text{-}C_5Me_5)_2]^{2+}$. The bridging olefin protons were observed as an AA′XX′ pattern at $\delta = 6.07$ and 6.63 ppm. From the simulation of the proton signals, $J_{2,3'} = 15.6$ and $J_{1,2} = J_{3,4} = 10.5$ Hz were obtained, indicating the *trans*-configuration of the central double bond in the bridging part. Since the $\eta\text{-}C_5Me_5$ ligand is sterically bulky, they seem to arrange in anti-parallel to each other in **9b**. Therefore, the structure of **9b** is represented as *anti-trans*-$[Ru_2(\mu_2\text{-}\eta^6\text{:}\eta^6\text{-}C_5H_4CHCH{=}CHCHC_5H_4)(\eta\text{-}C_5Me_5)_2]^{2+}[BF_4]_2$.

The ^1H NMR spectrum of **9a** in CD_3CN showed the presence of two isomers (ratio ca. 2:1). The number and the chemical shift of the proton signals for each isomer in **9a** are similar to each other, indicating that both isomers have a symmetrical plane or a center of symmetry and a similar

structure. The chemical shifts of the olefinic protons and the η-C_5H_4-ring protons in **9a** are very similar to those of the corresponding protons in **9b**. These features suggest that **9a** is an analogue of **9b** and that the two isomers in **9a** differ only in the arrangement of (η-C_5H_5)Ru moieties. The simulation of the olefinic proton signals in the main isomer of **9a** furnished the coupling constants similar to those observed in **9b**, implying that the central double bond in the bridging chain adopted a *trans* configuration. That is, their cations are formulated as *anti-trans*- and *syn-trans*-$[Ru_2(\mu_2\text{-}\eta^6\text{:}\eta^6\text{-}C_5H_4CHCH{=}CHCHC_5H_4)(\eta\text{-}C_5H_5)_2]^{2+}$. The presence of two isomers in **9a**, in contrast to **9b**, is likely due to the lesser sterical bulk of the (η-C_5H_5)Ru moiety compared with that of the (η-C_5Me_5)Ru moiety. A single crystal suitable for X-ray diffraction was obtained from the recrystallization of **9a** from CH_3NO_2/Et_2O. The ORTEP view of the cation in the obtained crystal is shown in Figure 4; selected bond lengths

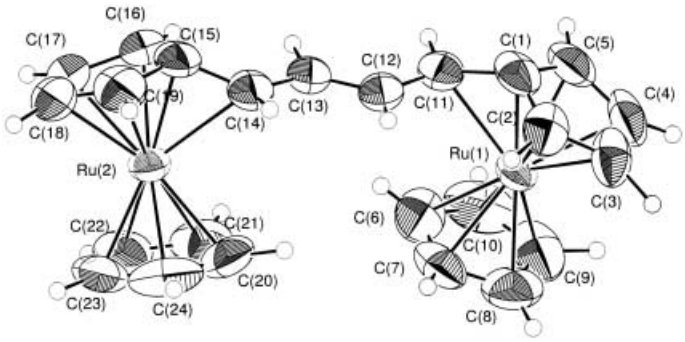

Figure 4. ORTEP view for the *syn* isomer of **9a**. Selected bond lengths [Å] and angles [°]: Ru(1)–C(1) = 2.054(7), Ru(1)–C(11) = 2.354(6), Ru(2)–C(14) = 2.358(7), Ru(2)–C(15) = 2.063(7), C(1)–C(11) = 1.407(11), C(11)–C(12) = 1.461(9), C(12)–C(13) = 1.336(8), C(13)–C(14) = 1.456(9), C(14)–C(15) = 1.409(11), C(1)-C(11)-C(12) = 123.0(6), C(11)-C(12)-C(13) = 122.2(6), C(12)-C(13)-C(14) = 122.0(6), C(13)-C(14)-C(15) = 122.3(6), C(11)-C(1)-Ctr(1) = 143.8(00), C(14)-C(15)-Ctr(2) = 143.1(00).

and angles are given in the figure legend. As seen in Figure 4, the cation in the obtained crystal has a *syn* arrangement of the (η-C_5H_5)Ru moiety, while complex **9a** exists as a mixture of *anti* and *syn* isomers in solution. The analyzed crystal was considered to be accidentally a crystal with the *syn* arrangement. The Ru(1)–C(11) (2.354(6) Å) and Ru(2)–C(14) (2.358(7) Å) bond lengths signify that the C(11) and C(14) atoms coordinate to the Ru atoms. The C(1)–C(11) (1.407(10) Å) and C(14)–C(15) (1.409(11) Å) distances are just as that of the double bond coordinated to metal. For reference, the corresponding Ru–C and C–C bond lengths in the fulvene complex, $[(\eta^6\text{-}C_5H_4CH_2)Ru(\eta\text{-}C_5H_5)]^+$, are 2.272(4) and 1.405(6) Å, respectively.[23] These features confirm the fulvene-complex structure of the (η-C_5H_5)Ru(C_5H_4CH) part in **9a**. The C(11)–C(12) (1.461(9) Å) and C(13)–C(14) bonds (1.456(9) Å) are single bonds and the C(12)–C(13) bond (1.336(8) Å) is a double bond in character. This bond alternation is in contrast to that of the corresponding bonding in (*E*,*E*)-**7a** [C(1)–C(2) (1.363(6) Å) and C(1)–C(1) (1.447(6) Å)]. The tilt angles of the C(1)–C(11) and C(15)–C(14) bonds from the η-C_5H_4 ring planes for *syn*-**9a** are 36.2° and 36.9°, respectively. These results definitely confirm that the structural rearrangement takes place in the oxidation of the neutral diene complex. It is also worthy to note that the central double bond C(12)=C(13) adopts an *E* configuration.

The ^{1}H NMR spectrum of **9c** in CD_3CN also showed the presence of two isomers (ratio ca. 2:1). The pattern of the proton signals for each isomer are much the same and the chemical shifts of the olefinic protons for each isomer are very similar to those of **9b**. The methyl-proton signals of the η-C_5Me_4-ring in **9c** appeared as two sets of separate four singlets, indicating that they are in an unsymmetrical environment. The protons of the Me groups in $[Ru_2(\mu_2\text{-}\eta^6\text{:}\eta^6\text{-}C_5Me_4CHCHC_5Me_4)(\eta\text{-}C_5H_5)_2]^{2+}$ were also reported to be observed as four signals.[19] These features suggest that **9c** involves a bis(fulvene)-complex structure and the two isomers differ only in the arrangement of the (η-C_5H_5)Ru moieties. That is, their cations are formulated as *anti-trans*- and *syn-trans*-$[Ru_2(\mu_2\text{-}\eta^6\text{:}\eta^6\text{-}C_5Me_4CHCH{=}CHCHC_5Me_4)(\eta\text{-}C_5H_5)_2]^{2+}$.

The ^{1}H NMR spectra of **10a** and **10b** in CD_3NO_2 bore a strong resemblance to those of **9a** and **9b**, respectively, except for the olefinic region; they also showed the presence of two isomers (ratio ca. 1:1 in **10a** and ca. 4:3 in **10b**). From the characteristics observed in the ring-proton signals for **10a** and **10b** and the similarity in the chemical shifts between their isomers, it is suggested that these complexes are higher analogues of **9a** and **9b**, respectively. The simulation of the olefinic proton signals in the main species of **10b** (CD_3NO_2) provided the coupling constants of $J_{2,3} = J_{4,5} =$ 15.8 Hz and $J_{1,2} = J_{3,4} = J_{5,6} =$ 10.6 Hz. So, the two double bonds in the bridging chain take a *trans*-configuration also in **10b**. The presence of two isomers in **10b** differs from that of one isomer in **9b**, and the decrease of the isomer ratio in **10a** (from ca. 2:1 for **9a** to ca. 1:1 for **10a**) seems to reflect the decreased steric repulsion between the terminal metal sites due to the elongation of the bridging oligoenes. Interestingly, the central double bond of the conjugating bridges in **9a**–**9c**, **10a**, and **10b** take a *trans* configuration, implying that the two isomers (**A** and **B**) observed in **9a**, **9c**, **10a**, and **10b** are considered to be generated from the s-*trans* conformers of the central single bond that connects the two double bond in **7a**, **7c**, **8a**, and **8b**, respectively. The isomers, **A** and **B**, are not conformational isomers. They come from the two conformers based on the C–C bond connecting the ruthenocene nucleus with the bridging olefin in **7** and **8**, respectively, before oxidation.

The cationic species **9b** and **10b** were reduced with Zn powder in CH_2Cl_2/MeCN (1:1) at room temperature to give the corresponding neutral complexes in quantitative yields, respectively. The ^{1}H NMR spectra of these products showed the formation of *E*,*E* and *E*,*E*,*E* isomers, respectively.

Complexes **7a**–**7c**, **8a**, and **8b** were oxidized in a chemically reversible process without an observable radical cation intermediate, although this redox reaction is electrochemically irreversible. Plausibly it can take place through the process shown in Scheme 5 for complex **7b**, which is similar to the square scheme proposed by Geiger.[16a,24] The process is composed of two simultaneous one-electron oxidations followed by a rapid chemical transformation (the structural

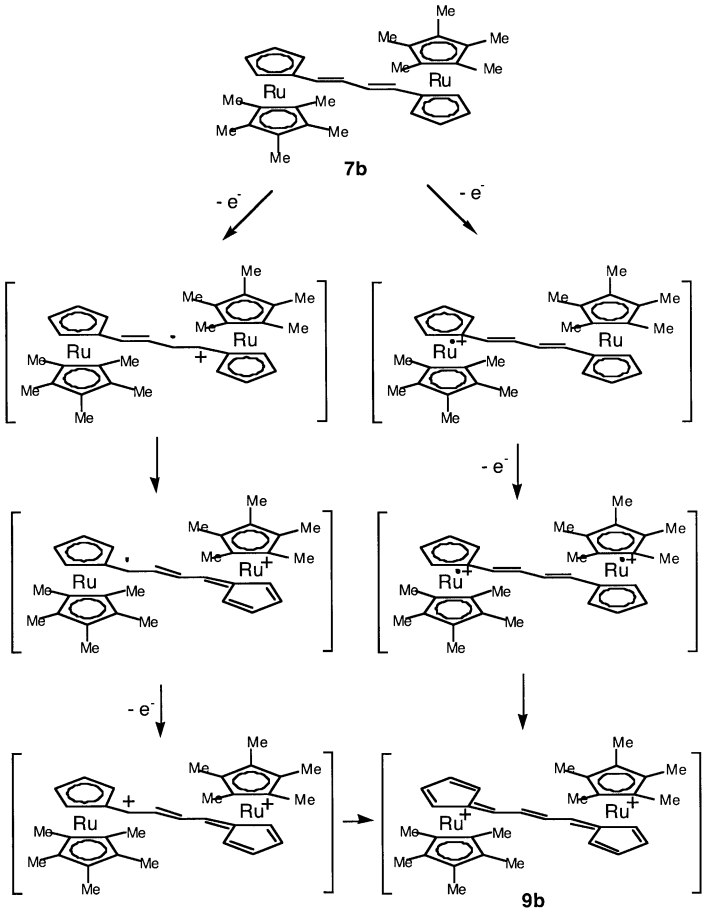

Scheme 5.

rearrangement). The first one-electron oxidation may be caused by the electron abstraction from the terminal metal sites or the bridging π bond. This produces an unstable radical cation that would lose another electron without delay. The stepwise rearrangement to a fulvene-complex structure or the spin-coupling of the diradical cation would lead to the bis(fulvene)-complex structure.

Taking previous results into consideration,[18,19] the two Ru sites in bis(ruthenocenyl) oligoenes, [Rc(CH=CH)$_n$Rc] (n=0–3), can sufficiently interact with little dependence on the elongation of the conjugation, and the two-electron-oxidized species can stabilized by the structural rearrangement to the dicationic complexes involving a bis(fulvene)-complex structure. This is very interesting, because the interaction between the two metal sites dramatically decreases with the extending conjugation in the one-electron-oxidized species of the bis(ferrocenyl) oligoenes, [Fc(CH=CH)$_n$Fc],[12a] and other dinuclear complexes bridged by oligoynes.[8,9] Moreover, the metal centers in the dication of dinuclear bis(ferrocenyl) complexes seem to behave as two noninteracting radical-cation sites, because the biferrocene dication has no significant exchange interaction between the two Fe^{III} centers.[25,26]

Theoretical study: For elucidating the electrochemical and structural properties, DFT calculations on the complexes [RcCH=CHRc], [Rc(CH=CH)$_2$Rc] (**7a**), and [Rc(CH=CH)$_3$Rc] (**8a**) were carried out. The molecular structures of all the complexes were fully optimized. The structural parameters obtained from the optimized structure of **7a** (Figure 5) are comparable with the crystallographically determined parameters for **7a**. For example, the C=C

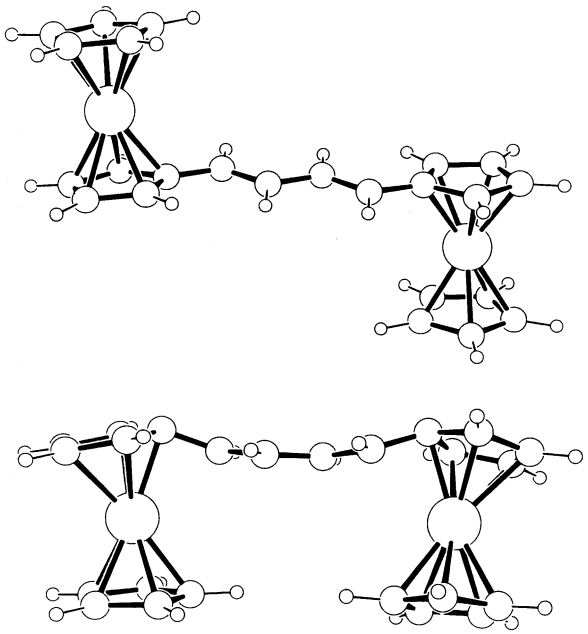

Figure 5. The optimized structures for **7a** (top) and **9a** (bottom).

(1.350 Å) and C–C bond lengths (1.440 Å) of the bridging butadiene moiety in the optimized structure are in an excellent agreement with the observed distances (1.363(6) Å for the C=C bond and 1.447(6) Å for the C–C bond) for **7a**. The Ru–C and C–C distances in the ruthenocene moiety of **7a** are also well reproduced (2.242 and 1.438 Å for the optimized structure and 2.188 (av) and 1.429 Å (av) for the observed structure, respectively). The result of the MO calculation showed that the HOMO has a roughly equal contribution from the ligand and the metal orbital and is antibonding in character, as seen in Figure 6. The contribution of the ligand orbital to the HOMO increased with the extending conjugation (n=1, 39.7; n=2, 53.0; n=3, 63.3%). These features are in good agreement with the qualitative anticipation based on the qualitative fragment orbital analysis between the metal d orbital of the ruthenocenyl parts and the π orbital of the bridging oligoene parts. The large contribution of the ligand orbital in the HOMO of RcCH=CHRc, **7a**, and **8a** may support the first one-electron extraction occurring at the bridging π-bond.

The energy level of the HOMO ascends in the following order, as seen in Figure 7: [RcCH=CHRc] (−0.18109 au) < [Rc(CH=CH)$_2$Rc] (**7a**) (−0.17716 au) < [Rc(CH=CH)$_3$Rc] (**8a**) (−0.17357 au). If electrochemical oxidation is assumed to involve the removal of an electron from the HOMO, the redox potentials of the complexes should decrease with the ascending HOMO energy. Indeed, this was the fact: [RcCH=CHRc] (+0.09 V) > [Rc(CH=CH)$_2$Rc] (**7a**) (−0.06 V) > [Rc(CH=CH)$_3$Rc] (**8a**) (−0.07 V).[27]

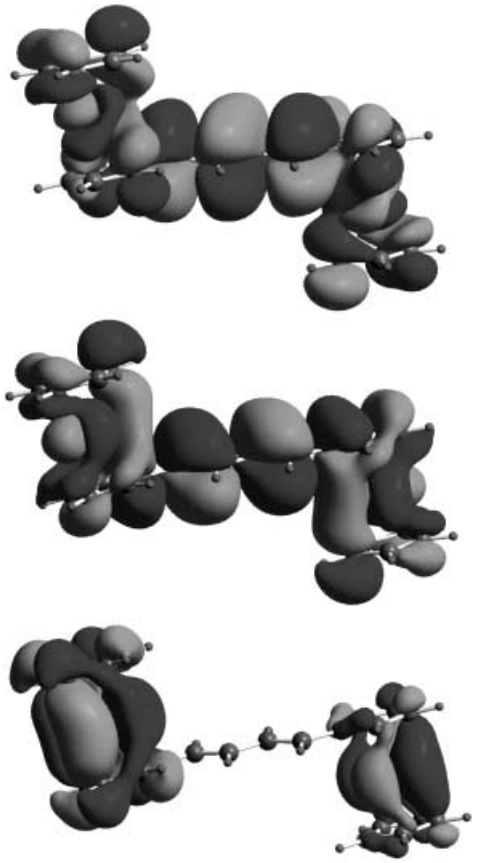

Figure 6. The LUMO (top), HOMO (middle), and HOMO−1 (bottom) for **7a**.

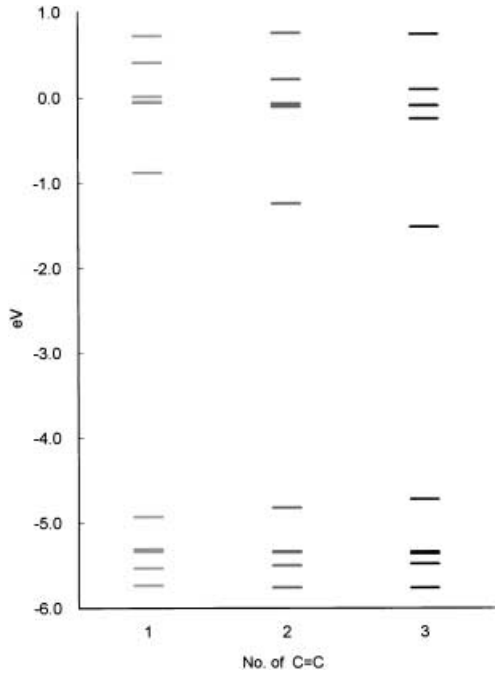

Figure 7. The MO energy diagram for $[Rc(CH{=}CH)_nRc]$ ($n=1$–3).

The HOMO energy of [Rc*CH=CHRc*] (−0.16884 au) was also calculated in order to evaluate the electronic effect of the methyl substituent. The energy is considerably higher than that of [RcCH=CHRc] (−0.18109 au), indicating the remarkable electron-donating effect of the methyl substituent and suggesting the potentially increased stability of the dicationic species.

The MO calculation for the two-electron-oxidized species of the ruthenocene-terminated oligoenes, $[RcCHCHRc]^{2+}$, $[Rc(CHCH)_2Rc]^{2+}$, and $[Rc(CHCH)_3Rc]^{2+}$, was also carried out. The geometry optimization reproduced considerably well the actual structure. For example, only a small difference (13.1 kJ mol^{-1}) in the total energy of the *anti* and *syn* isomers for $[Rc(CHCH)_2Rc]^{2+}$ was obtained, supporting the presence of two isomers, *anti*-**9a** and *syn*-**9a**. Moreover, a considerably correct fulvene-complex structure was reproduced in the ruthenocene part, as seen in Figure 5. The structural parameters obtained from the optimized structure for *syn*-$[Rc(CHCH)_2Rc]^{2+}$ are comparable with the crystallographically determined parameters for *syn*-**9a**. The Ru–C(α) and Ru–C(ipso) bond lengths are 2.53 and 2.16 Å (av), respectively, for the optimized structure and they are comparable with those found in the observed structure (2.354(6) and 2.358(7) Å, and 2.054(7) and 2.063(7) Å, respectively). The comparison of both interatomic distances suggests that the contribution of a bis(fulvene)-complex structure in the optimized structure is less than that in the observed structure, because the Ru–C(α) distance is longer and the Ru–C(ipso) distance is shorter in the former than in the latter. The C(α)–C(ipso) distance (1.40 Å) in the optimized structure is near that in the coordinated C=C bond and the similar bond lengths (1.409(11) and 1.407(10) Å) are observed for the corresponding bond of *syn*-**9a**. The central C=C (1.36 Å) and neighboring C–C bond lengths (1.44 Å) on the bridge in the optimized structure are also in considerable agreement with the observed distances for *syn*-**9a** (1.336(8) Å for the C=C bond and 1.461(9) and 1.456 (9) Å for the C–C bond). The tilt angle of the C(α)–C(ipso) bond from the η-C_5H_4 ring plane is 31.9° for the calculated $[Rc(CHCH)_2Rc]^{2+}$ and 36.2° and 36.9° for *syn*-**9a**. These parameters also support the lesser contribution of a bis(fulvene)-complex structure in the optimized structure. Similar structural characteristics are obtained from the calculation for the two-electron-oxidized species, $[RcCHCHRc]^{2+}$ and $[Rc(CHCH)_3Rc]^{2+}$.

Thus, the MO calculation for the oxidized species of such a series of ruthenocene-terminated oligoenes is very useful for the prediction of the structure and stability of the complexes. In the optimized structures, the Rc–C(α) bond lengths are elongated as follow: $[RcCHCHRc]^{2+}$ (2.47 Å) < $[Rc(CHCH)_2Rc]^{2+}$ (2.53 Å) < $[Rc(CHCH)_3Rc]^{2+}$ (2.55 Å) and the tilt angles of the C(ipso)–C(α) bond toward the C_5H_4 ring in *anti*-$[Rc(CHCH)_nRc]^{2+}$ decrease as follows: 34.0° ($n=1$) > 32.2° ($n=2$) > 31.5° ($n=3$). These parameters may suggest that the contribution of a bis(fulvene)-complex structure in the oxidized species decreases with the elongating conjugation and, hence, the stability of the oxidized species declines in the same order. This suggestion seems to be in agreement with the experimental facts.

Conclusion

Binuclear ruthenocene derivatives bridged by butadiene and hexatriene were newly prepared by the Wittig reaction of ruthenocenylmethylphosphonium salts with 3-ruthenocenyl-2-propenals and the Mukaiyama coupling of the propenals, respectively. Cyclic voltammetry showed that the ruthenocene-terminated oligoene derivatives, especially the pentamethylruthenocenyl series, underwent a stable two-electron redox process. Both neutral and oxidized species were air-stable and the redox process was chemically reversible. The structures of the two-electron-oxidized species were those of oligoene analogues of a bis(fulvene) complex. Therefore, the redox system $[Rc(CH{=}CH)_nRc]/[Rc(CHCH)_nRc]^{2+}$ may be regarded formally as a two-electron version of the FcH/FcH^+ system (Scheme 6). Their oxidation potentials appeared at lower potential (nearly equal to that of FcH) than that of the mononuclear ruthenocene derivatives and shifted to lower potential with the increasing CH=CH units. This is in remarkable contrast to those in the successive one-electron redox system. Since ruthenocene has well-developed derivative chemistry and the $[Rc(CH{=}CH)_nRc]$ system involves the Rc nucleus with versatile substitution, the $[Rc(CH{=}CH)_nRc]$ system may have a concealed potential for the development of novel materials. Such a work is in progress in our group.

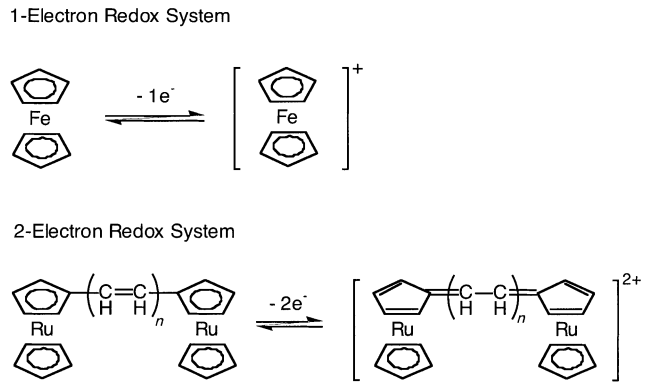

Scheme 6.

Experimental Section

Materials and methods: All reactions were carried out under an atmosphere of N_2 and/or Ar and workups were performed without precaution to exclude air. NMR spectra were recorded on Bruker AC300P, AM400, or ARX400 spectrometer. IR (ATR) spectra were recorded on Perkin–Elmer System 2000 spectrometer. Cyclic voltammetry was carried out by using BAS ALS600 in 10^{-1} M solution of nBu_4NClO_4 (polarography grade, Nacalai tesque) in CH_2Cl_2. CV cells were fitted with a glassy carbon (GC) working electrode, a Pt wire counter electrode and an Ag/Ag^+ pseudoreference electrode. The cyclic voltammograms were obtained at the scan rate of 0.1 Vs^{-1} in the 0.5–0.6 mmol solution of complexes. All potentials were represented vs FcH/FcH^+, which were obtained by the another measurement of ferrocene at the same conditions immediately after. Thin-layer coulometry were carried out on apparatus described earlier.[28] The simulation of the NMR spectra was carried out by the SwaN-MR software.[29] Solvents were purified by distillation from the drying agent prior to use as follows: CH_2Cl_2 ($CaCl_2$); $ClCH_2CH_2Cl$ ($CaCl_2$); CH_3CN (CaH_2); acetone ($CaSO_4$); THF (Na/benzophenone); diethyl ether ($LiAlH_4$). 1,2,3,4,5-Pentamethylruthenocene,[30] formylruthenocene (**1a**),[31] 1-formyl-1′,2′,3′,4′,5′-pentamethylruthenocene (**1b**),[19] 1-formyl-2,3,4,5-tetramethylruthenocene (**1c**),[19] 1-hydroxylmethylruthenocene (**5a**),[32] and 1-hydroxylmethyl-2,3,4,5-tetramethylruthenocene (**5c**)[19] were prepared according to the literatures. Other reagents were used as received from commercial suppliers.

Methyl (*E*)-3-ruthenocenylacrylate (2a): Carbomethoxymethylenetriphenylphosphorane (1.0 g, 3.0 mmol) was added to a solution of **1a** (0.78 g, 3.0 mmol) in dry benzene (30 mL) under N_2. The solution was refluxed for 24 h and then evaporated under reduced pressure. The residue was purifed by chromatography on SiO_2 by elution of CH_2Cl_2 to give methyl (*Z*)-3-ruthenocenylacrylate (52 mg, 5%) and methyl (*E*)-3-ruthenocenylacrylate (**2a**) (0.86 g, 90%) as yellow crystals. *E* isomer (**2a**): M.p. 120–121 °C; ^{1}H NMR (300 MHz, $CDCl_3$): $\delta = 3.74$ (s, 3H; OMe), 4.54 (s, 5H; η-C_5H_5), 4.69 (t, $J = 1.8$ Hz, 2H; η-C_5H_4), 4.86 (t, $J = 1.8$ Hz, 2H; η-C_5H_4), 5.97 (d, $J = 15.8$ Hz, 1H; 2-H), 7.44 ppm (d, $J = 15.8$ Hz, 1H; 3-H); ^{13}C NMR (75 MHz, $CDCl_3$): $\delta = 51.36$ (OMe), 70.34 (η-C_5H_4), 71.65 (η-C_5H_5), 72.19 (η-C_5H_4), 82.87 (η-C_5H_4-ipso), 114.09 (2-C), 144.29 (3-C), 167.67 ppm (CO); IR (ATR): $\tilde{\nu} = 1636$ (C=C), 1711 cm^{-1} (CO); elemental analysis calcd (%) for $C_{14}H_{14}O_2Ru$: C 53.33, H 4.48; found: C 53.78, H 4.41. *Z* isomer: M.p. 69–70 °C; ^{1}H NMR (300 MHz, $CDCl_3$): $\delta = 3.71$ (s, 3H; OMe), 4.54 (s, 5H; η-C_5H_5), 4.69 (t, $J = 1.8$ Hz, 2H; η-C_5H_4), 5.20 (t, $J = 1.8$ Hz, 2H; η-C_5H_4), 5.56 (d, $J = 15$ Hz, 1H; 2-H), 6.56 ppm (d, $J = 15$ Hz, 1H; 3-H); ^{13}C NMR (75 MHz, $CDCl_3$): $\delta = 51.04$ (OMe), 71.46 (η-C_5H_5), 72.13 (η-C_5H_4), 73.76 (η-C_5H_4), 81.88 (η-C_5H_4-ipso), 113.31 (2-C), 142.61 (3-C), 166.80 ppm (CO); IR (ATR): $\tilde{\nu} =$ 1627 (C=C), 1714 cm^{-1} (CO).

Methyl (*E*)-3-(1″,2″,3″,4″,5″-pentamethylruthenocenyl)acrylate (2b): This compound was prepared by a procedure similar to that described above for **2a** except for the reaction time of 70 h. Yellow crystals (93%); m.p. 90–91 °C; ^{1}H NMR (300 MHz, $CDCl_3$): $\delta = 1.84$ (s, 15H; Me), 3.75 (s, 3H; OMe), 4.37 (t, $J = 1.5$ Hz, 2H; η-C_5H_4), 4.40 (t, $J = 1.5$ Hz, 2H; η-C_5H_4), 5.79 (d, $J = 15.8$ Hz, 1H; 2-H), 7.23 ppm (d, $J = 15.8$ Hz, 1H; 3-H); ^{13}C NMR (75 MHz, $CDCl_3$): $\delta = 11.55$ (Me), 51.25 (OMe), 72.36 (η-C_5H_4), 75.25 (η-C_5H_4), 81.79 (η-C_5H_4-ipso), 86.11 (η-C_5Me_5), 111.60 (2-C), 144.71 (3-C), 168.17 ppm (CO); IR (ATR): $\tilde{\nu} = 1623$ (C=C), 1690 cm^{-1} (CO); elemental analysis calcd (%) for $C_{19}H_{24}O_2Ru$: C 59.20, H 6.28; found: C 59.42, H 6.34.

Methyl (*E*)-3-(2′,3′,4′,5′-tetramethylruthenocenyl)acrylate (2c): This compound was prepared by a procedure similar to that described above for **2a**. Yellow crystals (58%); m.p. 138–139 °C; ^{1}H NMR (300 MHz, $CDCl_3$): $\delta = 2.00$ (s, 6H; Me), 2.10 (s, 6H; Me), 3.75 (s, 3H; OMe), 4.25 (s, 5H; η-C_5H_5), 6.11 (d, $J = 16.0$ Hz, 1H; 2-H), 7.64 ppm (d, $J = 16.0$ Hz, 1H; 3-H); ^{13}C NMR (75 MHz, $CDCl_3$): $\delta = 11.01$ (Me), 13.18 (Me), 51.28 (OMe), 73.09 (η-C_5H_5), 80.53 (η-C_5H_4-ipso), 85.49 (η-C_5Me_4), 88.31 (η-C_5Me_4), 113.92 (2-C), 144.92 (3-C), 168.21 (CO); IR (ATR): $\tilde{\nu} = 1624$ (C=C), 1700 cm^{-1} (CO); elemental analysis calcd (%) for $C_{18}H_{22}O_2Ru$: C 58.21, H 5.97 ; Found: C 58.37, H 5.98 .

(*E*)-3-Ruthenocenylpropenol (3a): A solution of **2a** (0.27 g, 0.86 mmol) in THF (5 mL) was added dropwise to a suspension of $LiAlH_4$ (39 mg, 1.0 mmol) and $AlCl_3$ (34 mg, 0.25 mmol) in THF (5 mL) at 0 °C under Ar. The solution was stirred for 1 h at 0 °C and further for 2 h at room temperature. After hydrolysis with H_2O, the organic layer was separated. The aqueous layer was extracted with Et_2O. The organic layer and the extract were combined and then dried over $MgSO_4$. After evaporation, the residue was purifed by chromatography on SiO_2 to give **3a** as pale yellow crystals (0.18 g, 72%). M.p. 103–104 °C; ^{1}H NMR (300 MHz, $CDCl_3$): $\delta = 1.26$ (brs, 1H; OH), 4.12 (brt, 2H; CH_2), 4.51 (s, 5H; η-C_5H_5), 4.55 (t, $J = 1.5$ Hz, 2H; η-C_5H_4), 4.74 (t, $J = 1.5$ Hz, 2H; η-C_5H_4), 5.91 (dt, $J = 15.5$, 5.9 Hz, 2H; 2-H), 6.23 ppm (d, $J = 15.5$ Hz, 1H; 3-H); ^{13}C NMR (75 MHz, $CDCl_3$): $\delta = 63.80$ (OCH_2), 69.16 (η-C_5H_4), 70.49 (η-C_5H_4), 71.04 (η-C_5H_5), 86.59 (η-C_5H_4-ipso), 125.66 (=CH), 128.41 ppm (=CH); IR (ATR): $\tilde{\nu} = 1656$ (C=C), 3289 cm^{-1} (OH); elemental analysis calcd (%) for $C_{13}H_{14}ORu$: C 54.34, H 4.91; found: C 54.73, H 4.90.

(*E*)-3-(1″,2″,3″,4″,5″-Pentamethylruthenocenyl)-2-propenol (3b): This compound was prepared by a procedure similar to that described above for **3a**. Pale yellow crystals (73%); m.p. 95–96 °C; ^{1}H NMR (300 MHz,

$CDCl_3$): $\delta = 1.20$ (br, 1H; OH), 1.85 (s, 15H; Me), 4.16 (brt, 2H; CH_2), 4.23 (t, $J = 1.9$ Hz, 2H; η-C_5H_4), 4.27 (t, $J = 1.9$ Hz, 2H; η-C_5H_4), 5.79 (dt, $J = 15.6$, 6.3 Hz, 1H; 3-H), 6.01 ppm (d, $J = 15.6$ Hz, 1H; 2-H); ^{13}C NMR (75 MHz, $CDCl_3$): $\delta = 11.65$ (Me), 64.15 (OCH_2), 71.22 (η-C_5H_4), 73.29 (η-C_5H_4), 84.53 (η-C_5H_4-ipso), 85.11 (η-C_5Me_5), 124.08 (=CH), 128.66 ppm (=CH); IR (ATR): $\tilde{\nu} = 1657$ (C=C), 3288 cm^{-1} (OH); elemental analysis calcd (%) for $C_{18}H_{24}ORu$: C 60.48, H 6.76; found: C 60.46, H 6.67.

(*E*)-3-(2′,3′,4′,5′-Tetramethylruthenocenyl)-2-propenol (3c): This compound was prepared by a procedure similar to that described above for **3a**. Pale yellow crystals (72%); m.p. 113–114°C; ^{1}H NMR (300 MHz, $CDCl_3$): $\delta = 1.33$ (t, $J = 5.9$ Hz, 1H; OH), 1.97 (s, 6H; Me), 2.04 (s, 6H; Me), 4.20 (brt, 2H; OCH_2), 4.22 (s, 5H; η-C_5H_5), 5.95 (dt, $J = 16.2$, 5.9 Hz, 1H; 2-H), 6.43 ppm (dt, $J = 16.2$, 1.3 Hz, 1H; 3-H); ^{13}C NMR (75 MHz, $CDCl_3$): $\delta = 12.12$ (Me), 13.12 (Me), 64.66 (CH_2), 72.60 (η-C_5H_5), 84.25 (η-C_5Me_4-ipso), 84.62 (η-C_5Me_4), 86.44 (η-C_5Me_4), 127.88 (=C), 128.61 ppm (=C); IR (ATR): $\tilde{\nu} = 1652$ (C=C), 3276 cm^{-1} (OH); elemental analysis calcd (%) for $C_{17}H_{22}ORu$: C 59.46, H 6.46; found: C 59.60, H 6.50.

(*E*)-3-Ruthenocenylpropenal (4a): A mixture of **3a** (0.14 g, 5.0 mmol) and MnO_2 (1.50 g, 17.2 mmol) in dichloroethane (15 mL) was stirred for 4 h at room temperature. After the MnO_2 had been filtered off, the filtrate was evaporated and the residue was purified by chromatography on SiO_2 by elution of CH_2Cl_2 to afford **4a** as yellow crystals (0.13 g, 91%). M.p. 93–94°C; ^{1}H NMR (300 MHz, $CDCl_3$): $\delta = 4.56$ (s, 5H; η-C_5H_5), 4.91 (t, $J = 1.8$ Hz, 2H; η-C_5H_4), 4.74 (t, $J = 1.8$ Hz, 2H; η-C_5H_4), 6.27 (dd, $J = 15.5$, 8.0 Hz, 1H; 2-H), 7.30 (d, $J = 15.5$ Hz, 1H; 3-H), 9.48 ppm (d, $J = 8.0$ Hz, 1H; CHO); ^{13}C NMR (75 MHz, $CDCl_3$): $\delta = 70.75$ (η-C_5H_4), 71.99 (η-C_5H_5), 72.79 (η-C_5H_4), 82.20 (η-C_5H_4-ipso), 125.70 (2-C), 153.22 (3-C), 193.36 ppm (CO); IR (ATR): $\tilde{\nu} = 1618$ (C=C), 1663 cm^{-1} (CO); elemental analysis calcd (%) for $C_{13}H_{12}ORu$: C 54.73, H 4.24; found: C 54.86, H 4.16.

(*E*)-3-(1″,2″,3″,4″,5″-Pentamethylruthenocenyl)-2-propenal (4b): This compound was prepared by a procedure similar to that described above for **4a**. Yellow crystals (88%); m.p. 120–121°C; ^{1}H NMR (300 MHz, $CDCl_3$): $\delta = 1.82$ (s, 15H; Me), 4.45 (t, $J = 1.6$ Hz, 2H; η-C_5H_4), 4.47 (t, $J = 1.6$ Hz, 2H; η-C_5H_4), 6.11 (dd, $J = 15.5$, 8.1 Hz, 1H; 2-H), 7.00 (d, $J = 15.5$ Hz, 1H; 3-H), 9.49 ppm (d, $J = 8.1$ Hz, CHO); ^{13}C NMR (75 MHz, $CDCl_3$): $\delta = 11.32$ (Me), 72.73 (η-C_5H_4), 76.39 (η-C_5H_4), 81.42 (η-C_5H_4-ipso), 86.39 (η-C_5Me_5), 123.92 (2-C), 153.98 (3-C), 193.24 ppm (CO); IR (ATR): $\tilde{\nu} = 1610$ (C=C), 1652 cm^{-1} (CO); elemental analysis calcd (%) for $C_{18}H_{22}ORu$: C 60.83, H 6.24; found: C 60.76, H 6.19.

(*E*)-3-(2′,3′,4′,5′-Tetramethylruthenocenyl)-2-propenal (4c): This compound was prepared by a procedure similar to that described above for **4a**. Yellow crystals (82%); m.p. 138–139°C; ^{1}H NMR (300 MHz, $CDCl_3$): $\delta = 2.02$ (s, 6H; Me), 2.13 (s, 6H; Me), 4.27 (s, 5H; η-C_5H_5), 6.47 (dd, $J = 15.9$, 8.1 Hz, 1H; 2-H), 7.57 (d, $J = 15.9$ Hz, 1H; 3-H), 9.53 ppm (d, $J = 8.1$ Hz, 1H; CHO); ^{13}C NMR (75 MHz, $CDCl_3$): $\delta = 12.01$ (Me), 13.13 (Me), 73.38 (η-C_5H_5), 79.76 (η-C_5Me_4-ipso), 85.83 (η-C_5Me_4), 89.24 (η-C_5Me_4), 125.44 (2-C), 154.29 (3-C), 194.29 ppm (CHO); IR (ATR): $\tilde{\nu} = 1609$ (C=C), 1656 cm^{-1} (CO); elemental analysis calcd (%) for $C_{17}H_{20}ORu$: C 59.81, H 5.91; found: C 59.91, H 5.86.

(1″,2″,3″,4″,5″-Pentamethylruthenocenyl)methanol (5b): A solution of **1b** (0.56 g, 1.7 mmol) in THF (5 mL) was added dropwise to a suspension of $LiAlH_4$ (68 mg, 1.8 mmol) in THF (10 mL) at 0°C under N_2. The mixture was stirred for 1 h at 0°C and further for 2 h at room temperature. After ethyl acetate had been added, the mixture was poured into H_2O/EtOH/Et_2O (1/4/14), and then the resulting mixture was filtered under reduced pressure. The organic layer was separated from the filtrate, and the aqueous layer was extracted with Et_2O. The organic layer and the extract were combined and dried over $MgSO_4$. After evaporation, the residue was purified by chromatography on Al_2O_3 (deactivated with 10% H_2O) by elution of CH_2Cl_2 to give **5b** (0.51 g, 89%) as colorless crystals. M.p. 85–86°C; ^{1}H NMR (300 MHz, C_6D_6): $\delta = 1.17$ (t, $J = 5.7$ Hz, 1H; OH), 1.83 (s, 15H; Me), 4.05 (d, $J = 5.7$ Hz, 2H; CH_2), 4.06 (t, $J = 1.8$ Hz, 2H; η-C_5H_4), 4.20 ppm (t, $J = 1.8$ Hz, 2H; η-C_5H_4); ^{13}C NMR (75 MHz, C_6D_6): $\delta = 12.14$ (Me), 59.82 (CH_2), 72.36 (η-C_5H_4), 73.28 (η-C_5H_4), 85.26 (η-C_5Me_5), 92.52 ppm (η-C_5H_4-ipso); IR (ATR): $\tilde{\nu} = 3221$ cm^{-1} (OH); elemental analysis calcd (%) for $C_{16}H_{22}ORu$: C 57.99, H 6.69; found: C 58.16, H 6.72.

(Ruthenocenylmethyl)triphenylphosphonium bromide (6a): Triphenylphosphine hydrobromide (0.27 g, 0.77 mmol) was added to a solution of **5a** (0.20 g, 0.77 mmol) in dry toluene (25 mL). The solution was heated under reflux for 1 h. After cooling to room temperature, the resulting crystals were collected by filtration. The crystals were recrystallized from CH_2Cl_2/Et_2O to give pure **6a** (0.45 g, 99%) as colorless crystals. M.p. 207°C (decomp); ^{1}H NMR (300 MHz, $CDCl_3$): $\delta = 4.34$ (m, 2H; η-C_5H_4), 4.40 (t, $J = 1.8$ Hz, 2H; η-C_5H_4), 4.97 (d, $J_{PH} = 11.0$ Hz, 2H; CH_2), 7.62–7.82 ppm (m, 15H; Ph); ^{13}C NMR (75 MHz, $CDCl_3$): $\delta = 27.31$ (d, $J_{PC} = 44.1$ Hz, CH_2), 70.78 (η-C_5H_4), 71.94 (η-C_5H_5), 72.49 (η-C_5H_4), 76.18 (η-C_5H_4-ipso), 117.61 (d, $J_{PC} = 85.9$ Hz, Ph-ipso), 130.10 (d, $J_{PC} = 12.4$ Hz, Ph-*o*), 134.05 (d, $J_{PC} = 10.2$ Hz, Ph-*m*), 134.92 ppm (d, $J_{PC} = 3.4$ Hz, Ph-*p*); elemental analysis calcd (%) for $C_{29}H_{26}BrPRu$: C 59.32, H 4.35; found: C 59.39, H 4.47.

[(1″,2″,3″,4″,5″-Pentamethylruthenocenyl)methyl]triphenylphosphonium bromide (6b): This compound was prepared from **5b** by a procedure similar to that described above for **6a**. Colorless crystals; m.p. 179–180°C; ^{1}H NMR (300 MHz, $CDCl_3$): $\delta = 1.95$ (s, 15H; Me), 3.92 (m, 2H; η-C_5H_4), 4.05 (t, $J = 1.8$ Hz, 2H; η-C_5H_4), 4.49 (d, $J_{PH} = 11.0$ Hz, 2H; CH_2), 7.64–7.82 ppm (m, 15H; Ph); ^{13}C NMR (75 MHz, $CDCl_3$): $\delta = 11.96$ (Me), 26.35 (d, $J_{PC} = 42.7$ Hz, CH_2), 73.64 (η-C_5H_4), 74.50 (η-C_5H_4), 74.54 (η-C_5H_4-ipso), 86.12 (η-C_5Me_5), 117.88 (d, $J_{PC} = 84.2$ Hz, Ph-ipso), 130.14 (d, $J_{PC} = 13.4$ Hz, Ph-*o*), 134.29 (d, $J_{PC} = 9.8$ Hz, Ph-*m*), 134.97 ppm (d, $J_{PC} = 2.4$ Hz, Ph-*p*); elemental analysis calcd (%) for $C_{34}H_{36}BrPRu$: C 62.19, H 5.53; found: C 62.01, H 5.49.

[(2′,3′,4′,5′-Tetramethylruthenocenyl)methyl]triphenylphosphonium bromide (6c): This compound was prepared from **5c** by a procedure similar to that described above for **6a**. Colorless crystals; m.p. 182°C (decomp); ^{1}H NMR (300 MHz, $CDCl_3$): $\delta = 1.30$ (s, 6H; Me), 1.89 (s, 6H; Me),4.36 (s, 5H; η-C_5H_5), 4.78 (d, $J_{PH} = 9.9$ Hz, 2H; CH_2), 7.58–7.86 ppm (m, 15H; Ph); ^{13}C NMR (75 MHz, $CDCl_3$): $\delta = 12.03$ (Me), 12.45 (Me), 26.89 (d, $J_{PC} = 40.7$ Hz, CH_2), 73.45 (η-C_5H_5), 76.22 (η-C_5Me_4-ipso), 84.79 (η-C_5Me_4), 87.09 (η-C_5Me_4), 117.53 (d, $J_{PC} = 82.5$ Hz, Ph-ipso), 130.03 (d, $J_{PC} = 12.4$ Hz, Ph-*o*), 134.49 (d, $J_{PC} = 10.2$ Hz, Ph-*m*), 135.04 ppm (d, $J_{PC} = 3.4$ Hz, Ph-*p*); elemental analysis calcd (%) for $C_{33}H_{34}BrPRu$: C 61.68, H 5.33; found: C 61.48, H 5.25.

1,4-Bis(ruthenocenyl)butadiene (7a): A solution of LDA (0.80 mmol) in THF (5 mL) was added to a suspension of **6a** (0.47 g, 0.80 mmol) in THF (5 mL) at −80°C under Ar. The solution was stirred for 10 min and then a solution of **4a** (0.20 g, 0.72 mmol) in THF (5 mL) was added. The solution was warmed to room temperature and stirred for 1 h at room temperature and further refluxed for 3 h. After cooling, the precipitate was filtered and the filtrate was stirred with saturated aqueous NH_4Cl. The mixture was extracted with CH_2Cl_2 and dried over $MgSO_4$. After evaporation, the residue and the precipitate were combined and were purified by chromatography on Al_2O_3 (deactivated with 5% H_2O) with elution of hexane/benzene (4:1) to give a mixture (5:4) of (*E*,*E*)-**7a** and *E*,*Z* isomer (0.29 g, 78%) as pale yellow crystals. M.p. >250°C; elemental analysis calcd (%) for $C_{24}H_{22}Ru_2$: C 56.24, H 4.33; found: C 56.32, H 4.33. The repeated recrystallization of the mixture from benzene gave almost pure **7a**. (*E*,*E*)-**7a**: ^{1}H NMR (400 MHz, C_6D_6): $\delta = 4.42$ (s, 10H; η-C_5H_5), 4.49 (brs, 4H; η-C_5H_4), 4.76 (brs, 4H; η-C_5H_4), 6.15 (m, $J_{1,2} = 15.0$, $J_{1,3} = -0.4$, $J_{1,4} = 0.4$ Hz, 2H; $H_{1,4}$), 6.47 ppm (m, $J_{2,3} = 10.8$, $J_{2,4} = -0.4$ Hz, 2H; $H_{2,3}$); ^{13}C NMR (75 MHz, $CDCl_3$): δ 68.93 (η-C_5H_4), 70.53 (η-C_5H_4), 71.05 (η-C_5H_5), 87.82 (η-C_5H_4-ipso), 124.39 (=CH), 127.87 ppm (=CH); IR (ATR): $\tilde{\nu} = 1613$ cm^{-1} (C=C).

1,4-Bis(1″,2″,3″,4″,5″-pentamethylruthenocenyl)butadiene (7b). This compound was prepared from **4b** and **6b** by a procedure similar to that described above for **7a** and obtained as a mixture (3:2) of (*E*,*E*)-**7b** and the *E*,Z isomer as pale yellow crystals (46%). M.p. 209–210°C; elemental analysis calcd (%) for $C_{34}H_{42}Ru_2$: C 62.55, H 6.49; found: C 62.28, H 6.44. The repeated recrystallization of the mixture from benzene gave almost pure **7b**. (*E*,*E*)-**7b**: ^{1}H NMR (400 MHz, C_6D_6): $\delta = 1.88$ (s, 30H; Me), 4.26 (t, $J = 1.6$ Hz, 4H; η-C_5H_4), 4.36 (t, $J = 1.6$ Hz, 4H; η-C_5H_4), 5.93 (m, $J_{1,2} = 15.4$, $J_{1,3} = -0.8$, $J_{1,4} = 0.8$ Hz, 2H; $H_{1,4}$), 6.25 ppm (m, $J_{2,3} = 10.5$, $J_{2,4} = -0.8$ Hz, 2H; $H_{2,3}$); ^{13}C NMR (75 MHz, $CDCl_3$): $\delta = 11.70$ (Me), 70.96 (η-C_5H_4), 73.21 (η-C_5H_4), 85.22 (η-C_5Me_5), 86.48 (η-C_5H_4-ipso), 126.18 (=CH), 126.33 ppm (=CH); IR (ATR): $\tilde{\nu} = 1616$ cm^{-1} (C=C).

1,4-Bis(2′,3′,4′,5′-tetramethylruthenocenyl)butadiene (7c): This compound was prepared from **4c** and **6c** by a procedure similar to that described above for **7a** and obtained as a mixture (13:1) of (*E*,*E*)-**7c** and the *E*,Z isomer as pale yellow crystals (59%). M.p. >250°C; elemental analysis calcd (%) for $C_{32}H_{38}Ru_2$: C 61.52, H 6.13; found: C 61.73, H 6.11. The repeated recrystallization of the mixture from benzene gave almost pure **7c**. (*E*,*E*)-**7c**: ^{1}H NMR (400 MHz, C_6D_6): δ = 1.89 (s, 12H; Me), 2.10 (s, 12H; Me), 4.17 (s, 10H; η-C_5H_5), 6.69 (m, $J_{1,2}$ = 15.6, $J_{1,3}$ = −0.8, $J_{1,4}$ = 0.8 Hz, 2H; $H_{1,4}$), 6.85 ppm (m, $J_{2,3}$ = 10.6, $J_{2,4}$ = −0.8 Hz, 2H; $H_{2,3}$); ^{13}C NMR (75 MHz, $CDCl_3$): δ 12.23 (Me), 13.35 (Me), 72.60 (η-C_5H_5), 84.10 (η-C_5Me_4), 85.60 (η-C_5Me_4-ipso), 86.48 (η-C_5Me_4), 127.52 (=CH), 129.80 ppm (=CH); IR (ATR): $\tilde{\nu}$ = 1612 cm^{-1} (C=C).

(*E*,*E*,*E*)-1,6-Bis(ruthenocenyl)hexa-1,3,5-triene (8a): $TiCl_4$ (0.32 mL, 3.0 mmol) was added under Ar to a suspension of Zn dust (0.40 g, 6.0 mmol) in THF (15 mL) below −78°C. After stirring for 15 min, propenal **4a** (0.29 g, 1.0 mmol) was added to the mixture at the same temperature. The mixture was stirred for 20 min and then warmed gradually to room temperature. After stirring for 8 h at room temperature, the mixture was hydrolyzed with 10% aqueous Na_2CO_3. The reaction mixture was acidified (< pH 2) with 10% aqueous HCl solution. The resulting yellow crystals were collected with filtration and then dissolved in benzene. The solution was treated with activated carbon and then dried. The filtrate was extracted with CH_2Cl_2 and the extract was dried over $MgSO_4$. After evaporation, the residue was purified by chromatography on Al_2O_3 (deactivated with 10% H_2O) to give yellow crystals. Total yield: 78 mg (29%); m.p. 245°C (decomp); ^{1}H NMR (400 MHz, $CDCl_3$): δ = 4.50 (s, 10H; η-C_5H_5), 4.58 (t, J = 1.6 Hz, 4H; η-C_5H_4), 4.77 (t, J = 1.6 Hz, 4H; η-C_5H_4), 6.15 (m, $J_{3,4}$ = 15.4, $J_{3,5}$ = −0.2, $J_{3,6}$ = 0.2 Hz, 2H; $H_{3,4}$), 6.17 (m, $J_{1,2}$ = 15.4, $J_{1,3}$ = −0.2, $J_{1,4}$ = 0.2 Hz, 2H; $H_{1,6}$), 6.35 ppm (m, $J_{2,3}$ = 10.3, $J_{2,4}$ = −0.2, $J_{2,5}$ = 0.2 Hz, 2H; $H_{2,5}$); ^{13}C NMR (75 MHz, $CDCl_3$): δ = 69.00 (η-C_5H_4), 70.67 (η-C_5H_4), 71.13 (η-C_5H_5), 87.61 (η-C_5H_4-ipso), 126.95 (=CH), 129.04 (=CH), 131.39 ppm (=CH); IR (ATR): $\tilde{\nu}$ = 1626 cm^{-1} (C=C); elemental analysis calcd (%) for $C_{26}H_{24}Ru_2$: C 57.98, H 4.49; found: C 58.11, H 4.44.

(*E*,*E*,*E*)-1,6-Bis(1″,2″,3″,4″,5″-pentamethylruthenocenyl)hexa-1,3,5-triene (8b): This compound was prepared from **4b** by a procedure similar to that described above for **8a**. Yellow crystals (32%); m.p. 238°C (decomp); ^{1}H NMR (400 MHz, C_6D_6): δ = 1.83 (s, 30H; Me), 4.25 (t, J = 1.6 Hz, 4H; η-C_5H_4), 4.34 (t, J = 1.6 Hz, 4H; η-C_5H_4), 6.03 (m, $J_{1,2}$ = 15.8, $J_{1,3}$ = −0.9, $J_{1,4}$ = 0.9 Hz, 2H; $H_{1,6}$), 6.35 (m, $J_{3,4}$ = 15.8, $J_{3,5}$ = −0.9, $J_{3,6}$ = 0.9 Hz, 2H; $H_{3,4}$), 6.42 ppm (m, $J_{2,3}$ = 10.6, $J_{2,4}$ = −0.9, $J_{2,5}$ = 0.9 Hz, 2H; $H_{2,5}$); ^{13}C NMR (75 MHz, $CDCl_3$): δ = 11.70 (Me), 71.05 (η-C_5H_4), 73.39 (η-C_5H_4), 85.37 (η-C_5Me_5), 87.61 (η-C_5H_4-ipso), 125.85 (=CH), 128.15 (=CH), 130.87 ppm (=CH); IR (ATR): $\tilde{\nu}$ = 1630 cm^{-1} (C=C); elemental analysis calcd (%) for $C_{36}H_{44}Ru_2$: C 63.69, H 6.53; found: C 64.09, H 6.71.

(*E*,*E*,*E*)-1,6-Bis(2′,3′,4′,5′-tetramethylruthenocenyl)hexa-1,3,5-triene (8c): This compound was prepared from **4c** by a procedure similar to that described above for **8a**. Yellow crystals (57%); m.p. 234°C (decomp); ^{1}H NMR (400 MHz, C_6D_6): δ = 1.91 (s, 12H; Me), 2.10 (s, 12H; Me), 4.21 (s, 10H; η-C_5H_5), 6.38 (m, $J_{3,4}$ = 15.4, $J_{3,5}$ = −0.4, $J_{3,6}$ = 0.4 Hz, 2H; $H_{3,4}$), 6.58 (m, $J_{1,2}$ = 15.4, $J_{1,3}$ = −0.4, $J_{1,4}$ = 0.4 Hz, 2H; $H_{1,6}$), 6.72 ppm (m, $J_{2,3}$ = 10.5, $J_{2,4}$ = −0.4, $J_{2,5}$ = 0.4 Hz, 2H; $H_{2,5}$); ^{13}C NMR ($CDCl_3$, 75 MHz): δ 12.20 (Me), 13.27 (Me), 72.66 (η-C_5H_5), 84.19 (η-C_5Me_4), 85.37 (η-C_5Me_4-ipso), 86.71 (η-C_5Me_4), 128.64 (=CH), 129.50 (=CH), 131.79 ppm (=CH); IR (ATR): $\tilde{\nu}$ = 1626 cm^{-1} (C=C); elemental analysis calcd (%) for $C_{34}H_{40}Ru_2$: C 62.74, H 6.20; found: C 62.96, H 6.18.

Chemical oxidation—[Ru_2(μ$_2$-η^6:η^6-C_5H_4CHCH=CHCHC$_5$H$_4$)(η-C_5H_5)$_2$][BF_4]$_2$ (9a). A solution of the butadiene (**7a**) (15.4 mg, 0.03 mmol) and *p*-benzoquinone (6.3 mg, 0.06 mmol) in CH_2Cl_2 (5 mL) was cooled to 0°C. one drop of BF_3·OEt_2 was added to this solution, and the resulting dark red solution was stirred for 3 h at the same temperature. After dry diethyl ether (5 mL) had been added to the solution, the mixture was stirred for 1 h and then resulting precipitates were collected by filtration. Recrystallization from CH_3CN/Et_2O by the diffusion method in freezer gave deep red crystals (20.5 mg, 96%). M.p. 180°C; elemental analysis calcd (%) for $C_{24}H_{22}B_2F_8Ru_2$: C 42.01, H 3.23; found: C 42.22, H 3.07. This was a mixture of two isomers, **A** and **B** (ca. 2:1) by the ^{1}H NMR spectrum. The following NMR data were extracted from the NMR spectrum of the mixutre. Isomer **A**: ^{1}H NMR (400 MHz, CD_3NO_2,): δ = 5.28 (m, 2H; η-C_5H_4), 5.39 (s, 10H; η-C_5H_5), 5.89 (br d, J = 2.8 Hz, 2H; η-C_5H_4), 6.23 (dt, J = 2.7, 1.1 Hz, η-C_5H_4), 6.38 (m, 2H; η-C_5H_4), 6.77 (m, $J_{1,2}$ = 11.3, $J_{1,3}$ = −0.9, $J_{1,4}$ = 0.9 Hz, 2H; $H_{1,4}$), 6.87 ppm (m, $J_{2,3}$ = 14.6, $J_{2,4}$ = −0.9, $J_{3,4}$ = 11.3 Hz, 2H; $H_{2,3}$); ^{13}C NMR (75 MHz, CD_3CN): δ = 83.66 (η-C_5H_4), 84.66 (η-C_5H_4), 87.07 (η-C_5H_4), 92.88 (=CH), 93.33 (η-C_5H_4), 97.77 (η-C_5H_4), 104.22 (η-C_5H_4-ipso), 136.38 ppm (=CH). Isomer **B**: ^{1}H NMR (400 MHz, CD_3NO_2): δ = 5.31 (m, 2H; η-C_5H_4), 5.36 (s, 10H; η-C_5H_5), 5.83 (br d, J = 2.9 Hz, 2H; η-C_5H_4), 6.26 (m, 2H; η-C_5H_4), 6.31 (m, 2H; η-C_5H_4), 6.68 (m, 2H; $H_{1,4}$), 6.80 ppm (m, 2H; $H_{2,3}$); ^{13}C NMR (75 MHz, CD_3CN): δ = 83.88 (η-C_5H_4), 84.41 (η-C_5H_4), 86.90 (η-C_5H_5), 93.14 (=CH), 93.29 (η-C_5H_4), 98.02 (η-C_5H_4), 104.13 (η-C_5H_4-ipso), 136.27 ppm (=CH).

[Ru_2(μ$_2$-η^6:η^6-C_5H_4CHCH=CHCHC$_5$H$_4$)(η-C_5Me_5)$_2$][BF_4]$_2$ (9b): This compound was prepared from **7b** by a procedure similar to that described above for **9a**. Red-violet crystals (85%). M.p. >250°C; elemental analysis calcd (%) for $C_{34}H_{42}B_2F_8Ru_2$: C 49.42, H 5.20; found: C 49.65, H 5.08. This was a single isomer by the ^{1}H NMR spectrum. ^{1}H NMR (400 MHz, CD_3NO_2): δ = 1.97 (s, 30H; Me), 4.97 (br d, J = 2.9 Hz, 2H; η-C_5H_4), 5.51 (br d, J = 2.9 Hz, 2H; η-C_5H_4), 5.85 (dt, J = 2.9, 1.1 Hz, 2H; η-C_5H_4), 5.94 (br t, J = 2.9 Hz, 2H; η-C_5H_4), 6.07 (m, $J_{1,2}$ = 10.5, $J_{1,3}$ = −0.8, $J_{1,4}$ = 0.8 Hz, 2H; $H_{1,4}$), 6.63 ppm (m, $J_{2,3}$ = 15.6, $J_{2,4}$ = −0.8, $J_{3,4}$ = 10.5 Hz, 2H; $H_{2,3}$); ^{13}C NMR (100 MHz, CD_3CN): δ = 10.58 (Me), 80.81 (η-C_5H_4), 83.58 (η-C_5H_4), 96.62 (η-C_5H_4), 97.29 (η-C_5H_4), 100.13 (=CH), 101.59 (η-C_5Me_5), 105.78 (η-C_5H_4-ipso), 135.39 ppm (=CH).

The same product was also obtained by the oxidation of **7b** with $AgBF_4$.

Complex **9b** (7.7 mg, 0 009 mmol) was stirred with Zn dust (30 mg) for 1 h in CH_2Cl_2 (1 mL) and CH_3CN (1 mL). The mixture was filtered and the filtrate was evaporated under reduced pressure. The residue was purified by chromatography on silica gel by elution of benzene to give the neutral complex (*E*,*E*)-**7b** (6.1 mg) qunatitatively.

[Ru_2(μ$_2$-η^6:η^6-C_5Me_4CHCH=CHCHC$_5$Me$_4$)(η-C_5H_5)$_2$][BF_4]$_2$ (9c): This compound was prepared from **7c** by a procedure similar to that described above for **9a**. Orange crystals (89%); m.p. >235°C (decomp); elemental analysis calcd (%) for $C_{32}H_{38}B_2F_8Ru_2$: C 48.14, H 4.80; found: C 48.39, H 4.79. This was a mixture of two isomers, **A** and **B** (ca. 2:1) by the ^{1}H NMR spectrum. The following NMR data were extracted from the NMR spectrum of the mixutre. Isomer **A**: ^{1}H NMR (400 MHz, CD_3NO_2): δ = 1.87 (s, 6H; Me), 2.18 (s, 6H; Me), 2.27 (s, 6H; Me), 2.31 (s, 6H; Me), 5.11 (s, 10H; η-C_5H_5), 6.82 (m, $J_{1,2}$ = 11.6, $J_{1,3}$ = −0.9, $J_{1,4}$ = 0.9 Hz, 2H; $H_{1,4}$), 7.34 ppm (m, $J_{2,3}$ = 14.8, $J_{2,4}$ = −0.9, $J_{3,4}$ = 11.6 Hz, 2H; $H_{2,3}$); ^{13}C NMR (75 MHz, CD_3CN): δ = 9.88 (2 Me), 11.63 (Me), 11.73 (Me), 88.18 (η-C_5H_5), 95.16 (=CH), 99.03 (η-C_5Me_4-ipso), 99.98 (η-C_5Me_4), 100.19 (η-C_5Me_4), 107.96 (η-C_5Me_4), 109.16 (η-C_5Me_4), 134.88 ppm (=CH). Isomer **B**: ^{1}H NMR (400 MHz, CD_3NO_2): δ = 1.87 (s, 6H; Me), 2.22 (s, 6H; Me), 2.25 (s, 6H; Me), 2.27 (s, 6H; Me), 5.06 (s, 10H; η-C_5H_5), 6.68 (m, 2H; $H_{1,4}$), 7.21 ppm (m, 2H; $H_{2,3}$); ^{13}C NMR (75 MHz, CD_3CN): δ = 11.63 (Me), 11.69 (Me), 12.62 (Me), 12.89 (Me), 88.06 (η-C_5H_5), 95.64 (=CH), 99.29 (η-C_5Me_4-ipso), 99.98 (η-C_5Me_4), 100.19 (η-C_5Me_4), 108.31 (η-C_5Me_4), 109.31 (η-C_5Me_4), 135.48 ppm (=CH).

[Ru_2(μ$_2$-η^6:η^6-C_5H_4CHCH=CHCH=CHCHC$_5$H$_4$)(η-C_5H_5)$_2$][BF_4]$_2$ (10a): This compound was prepared from **8a** by a procedure similar to that described above for **9a**. Red-violet crystals (50%); m.p. 180°C (decomp); elemental analysis calcd (%) for $C_{26}H_{24}B_2F_8Ru_2$: C 43.85, H 3.40; found: C 43.48, H 3.21. This was a ca. 1:1 mixture of two isomers by the ^{1}H NMR spectrum. ^{1}H NMR (400 MHz, CD_3CN): δ = 5.14 (m, 4H; η-C_5H_4), 5.23 (s, 10H; η-C_5H_5), 5.25 (s, 10H; η-C_5H_5), 5.76 (m, 4H; η-C_5H_4), 6.08 (m, 4H; η-C_5H_4), 6.24 (m, 4H; η-C_5H_4), 6.41 (m, 4H; =CH), 6.82 ppm (m, 4H; =CH), 7.01 (m, 4H; =CH); ^{13}C NMR (75 MHz, CD_3CN): δ = 83.30 (η-C_5H_4), 83.84 (η-C_5H_4), 83.87 (η-C_5H_4), 86.59 (η-C_5H_5), 86.62 (η-C_5H_5), 92.28 (=CH), 92.31 (=CH), 92.63 (η-C_5H_4), 92.67 (η-C_5H_4), 101.87 (η-C_5H_4), 101.94 (η-C_5H_4), 102.78 (η-C_5H_4-ipso), 102.92 (η-C_5H_4-ipso), 134.11 (=CH), 134.20 (=CH), 140.18 (=CH), 140.33 ppm (=CH).

[Ru_2(μ$_2$-η^6:η^6-C_5H_4CHCH=CHCH=CHCHC$_5$H$_4$)(η-C_5Me_5)$_2$][BF_4]$_2$ (10b): This compound was prepared from **8b** by a procedure similar to that described above for **9a**. Red-violet crystals (73%); m.p. >250°C; elemental analysis calcd (%) for $C_{36}H_{44}B_2F_8Ru_2$: C 50.72, H 5.20; found: C 50.35, H 5.04. This was a mixture of two isomers, **A** and **B** (ca. 4:3) by the ^{1}H NMR spectrum. The following NMR data were extracted from the NMR spectrum of the mixutre. Isomer **A**: ^{1}H NMR (400 MHz,

CD_3NO_2): $\delta = 1.97$ (s, 30H; Me), 4.92 (br d, 4H; η-C_5H_4), 5.47 (br d, 4H; η-C_5H_4), 5.78 (br t, 4H; η-C_5H_4), 5.90 (m, 4H; η-C_5H_4), 6.18 (m, $J_{1,2} = 10.6$, $J_{1,3} = -0.7$, $J_{1,4} = 0.7$ Hz, 2H; $H_{1,6}$), 6.45 (m, $J_{2,3} = 15.8$, $J_{2,4} = -0.7$, $J_{2,5} = 0.7$, $J_{5,6} = 10.6$ Hz, 2H; $H_{2,5}$), 7.20 ppm (m, $J_{3,4} = 10.6$, $J_{3,5} = -0.7$, $J_{3,6} = 0.7$, $J_{4,5} = 15.8$ Hz, 2H; $H_{3,4}$); ^{13}C NMR (75 MHz, CD_3CN): $\delta = 10.50$ (Me), 80.28 (η-C_5H_4), 80.12 (η-C_5H_4), 96.21 (2 η-C_5H_4), 99.35 (=CH), 104.93 (η-C_5H_4-ipso), 105.86 (η-C_5Me_5), 133.68 (=CH), 139.81 ppm (=CH). Isomer **B**: ^{1}H NMR (400 MHz, CD_3CN): $\delta = 1.63$ (s, 30H; Me), 4.92 (br d, 2H; η-C_5H_4), 5.45 (br d, 2H; η-C_5H_4), 5.78 (br t, 2H; η-C_5H_4), 5.90 (m, 2H; η-C_5H_4), 6.16 (m, 2H; $H_{1,6}$), 6.41 (m, 2H; =CH), 7.16 ppm (m, 2H; =CH); ^{13}C NMR (75 MHz, CD_3CN): $\delta = 10.48$ (Me), 80.32 (η-C_5H_4), 83.20 (η-C_5H_4), 96.21 (η-C_5H_4), 86.77 (η-C_5H_4), 99.64 (=CH), 104.88 (η-C_5H_4-ipso), 105.61 (η-C_5Me_5), 133.32 (=CH), 139.70 ppm (=CH).

Complex **10b** was reduced with Zn dust by a procedure similar to that described in the section of **9b** to give (*E*,*E*,*E*)-**8b** in a quantitative yield.

MO calculations: DFT calculations were performed with Gaussian 98 program[33] running on the workstations assembled by HIT Inc. The enediyl-, dienediyl-, and trienediyl-bridged binuclear ruthenocenes and their two-electron-oxidized species were optimized fully using a standard 3-21G(d) basis set and B3LYP functional, which incorporates the three-parameter exchange functional by Becke[34] with the correlation functional by Lee, Yang, and Parr[35] (B3LYP3–21G(d)). Molecular orbital energy levels, together with the orbital diagrams, were obtained from B3LYP3-21G(d) calculations. The graphic representations of the calculated molecular orbitals were obtained using GaussViewW.[36]

Structure determinations: The crystallographic data are listed in Table 4 for **7a** and **9a**. Data collection of crystal data for **7a** and **9a** were performed at room temperature on Mac Science MXC18 K diffractometer and Mac Science DIP3000 image processor with grafite monochromated $Mo_{K\alpha}$ radiation ($\lambda = 0.71073$ Å) and an 18 kW rotating anode generator, respectively. The structures were solved with the Dirdif–Patty method in MAXUS (software-package fro structure determination) and refined finnaly by full-matrix least-squares procedure with SHELEX. Absorption correction for **7a** and **9a** with the ψ-scan method and the Sotav method, respectively, and anisotropic refinement for non-hydrogen atom were carried out. The hydrogen atoms, located from difference Fourier maps or calculation, were refined isotropically.

Table 4. Crystallographic data for **7a** and **9a**.

	7a	**9a**
formula	$C_{24}H_{22}Ru_2$	$C_{24}H_{22}B_2F_8Ru_2$
M_r	512.58	686.19
crystal system	monoclinic	triclinic
space group	$P2_1/c$	$P\bar{1}$
a [Å]	5.750(2)	7.9020(6)
b [Å]	14.442(4)	7.9070(7)
c [Å]	11.431(4)	19.790(2)
α [°]		91.559(5)
β [°]	102.57(3)	91.854(5)
γ [°]		101.862(4)
V [Å^3]	926.5(5)	1208.7(2)
Z	2	2
ρ_{calcd} [Mg m^{-3}]	1.837	1.885
size [mm]	$0.50 \times 0.08 \times 0.08$	$0.35 \times 0.08 \times 0.08$
index range	$0 \le h \le 7$	$10 \le h \le 10$
	$-18 \le k \le 0$	$-10 \le k \le 10$
	$-14 \le l \le 14$	$0 \le l \le 24$
reflections measured	2437	4447
unique reflections	2066	4438
μ [mm^{-1}]	1.634	1.323
reflections observed [$(I) > 2\sigma(I)$]	2066	4438
parameters	58	325
R	0.044	0.057
Rw	0.195	0.170
S	2.588	1.144
max/min electon density [e Å^{-3}]	1.196/−1.849	1.233/−1.134

CCDC-225203 (**7a**) and CCDC-225204 (**9a**) contain the supplementary crystallographic data for this paper. These data can be obtained free of charge via www.ccdc.cam.ac.uk/conts/retrieving.html (or from the Cambridge Crystallographic Data Centre, 12, Union Road, Cambridge CB21EZ, UK; fax: (+44)1223–336–033; or e-mail: deposit@ccdc.cam.ac.uk).

Acknowledgement

The present work was supported by Grant-in-Aid for Science Research (No. 10640538) from the Ministry of Education, Science, and Culture of Japan.

[1] K. Deuchert, S. Hünig, *Angew. Chem.* **1978**, *90*, 927; *Angew. Chem. Int. Ed. Engl.* **1978**, *17*, 875.
[2] a) W. E. Geiger, N. G. Connelly, *Adv. Organomet. Chem.* **1985**, 24, 87–130; b) W. Beck, B. Niemer, Wieser, *Angew. Chem.* **1993**, *105*, 969; *Angew. Chem. Int. Ed. Engl.* **1993**, *32*, 923; c) H. Lang, *Angew. Chem.* **1994**, *106*, 569; *Angew. Chem. Int. Ed. Engl.* **1994**, *33*, 547; d) A. Nakamura, *Bull. Chem. Soc. Jpn.* **1995**, *68*, 1515; e) N. J. Long, *Angew. Chem.* **1995**, *107*, 37; *Angew. Chem. Int. Ed. Engl.* **1995**, *34*, 21; f) U. H. Bunz, *Angew. Chem.* **1996**, *108*, 1047; *Angew. Chem. Int. Ed. Engl.* **1996**, *35*, 969; f) N. J. Long, C. K. Williams, *Angew. Chem.* **2003**, *115*, 2690; *Angew. Chem. Int. Ed.* **2003**, *42*, 2586.
[3] D. Astruc, *Electron Transfer and Radical Process in Transition-metal Chemistry*, VCH, New York, **1995**.
[4] *Mixed-Valence Compounds* (Ed.: D. H. Brown), Reidel, Dordrecht, **1980**.
[5] A. Togni, T. Hayashi, *Ferrocenes*, VCH, New York, **1995**.
[6] F. Paul, C. Lapinte, *Coord. Chem. Rev.* **1998**, *178–180*, 431.
[7] N. J. Long, C. K. Williams, *Angew. Chem.* **2003**, *115*, 2690; *Angew. Chem. Int. Ed.* **2003**, *42*, 2586.
[8] a) J. W. Seyler, W. Weng, Y. Zhou, J. A. Gladysz, *Organometallics* **1993**, *12*, 3802; b) Y. Zhou, J. W. Seyler, W. Weng, A. M. Arif, J. A. Gladysz, *J. Am. Chem. Soc.* **1993**, *115*, 8509; c) M. Brady, W. Weng, Y. Zhou, J. W. Seyler, A. J. Amoroso, A. M. Arif, M. Böhme, G. Frenking, J. A. Gladysz, *J. Am. Chem. Soc.* **1997**, *119*, 775; d) M. Brady, W. Weng, J. A. Gladysz, *J. Chem. Soc. Chem. Commun.* **1994**, 2655; e) T. Bartik, B. Bartik, M. Brady, R. Dembinski, J. A. Gladysz, *Angew. Chem.* **1996**, *108*, 467; *Angew. Chem. Int. Ed. Engl.* **1996**, *35*, 414; f) R. Dembinski, T. Bartik, B. Bartik, M. Jaeger, J. A. Gladysz, *J. Am. Chem. Soc.* **2000**, *122*, 810.
[9] a) N. Le Narvor, C. Lapinte, *J. Chem. Soc. Chem. Commun.* **1993**, 357; b) N. Le Narvor, L. Troupet, C. Lapinte, *J. Am. Chem. Soc.* **1995**, *117*, 7129; c) F. Coat, C. Lapinte, *Organometallics* **1996**, *15*, 477; d) N. Le Narvor, C. Lapinte, *Organometallics*, **1995**, *14*, 634; e) M. Guillemot, L. Troupet, C. Lapinte, *Organometallics* **1998**, *17*, 1928.
[10] a) B. A. Etzenhouser, M. D. Cavanaugh, H. N. Spurgeon, M. B. Sponsler, *J. Am. Chem. Soc.* **1994**, *116*, 2221; b) B. A. Etzenhouser, Q. Chen, M. B. Sponsler, *Organometallics* **1994**, *13*, 4176; c) M. B. Sponsler, *Organometallics* **1995**, *14*, 1920; d) V. Guillaume, V. Mahias, A. Mari, C. Lapinte, *Organometallics* **2000**, *19*, 1422; e) M.-C. Chung, X. Gu, B. A. Etzenhouser, A. M. Spuches, P. T. Rye, S. K. Seetharaman, D. J. Rose, J. Zubieta, M. B. Sponsler, *Organometallics* **2003**, *22*, 3485.
[11] S. H. Liu, H. Xia, T. B. Wen, Z. Zhou, G. Jia, *Organometallics* **2003**, *22*, 737.
[12] a) A.-C. Ribou, J.-P. Launay, M. L. Sachtleben, H. Li, C. W. Spangler, *Inorg. Chem.* **1996**, *35*, 3735; b) Y. J. Chen, D.-S. Pan, C.-F. Chiu, J.-X . Su, S. J. Lin, K. S. Kwan, *Inorg. Chem.* **2000**, *39*, 953; c) H.-H. Wei, C.-Y. Lin, S.-J. Chang, *Proc. Natl. Sci. Counc. Repub. China Part B* **1983**, *7*, 35; d) S. I. Amer, G. Sadler, P. M. Henry, G. Ferguson, G. L. Ruhl, *Inorg. Chem.* **1985**, *24*, 1517.

[13] M. I. Bruce, P. Hinterding, R. T. Tiekink, B. W. Skelton, A. H. White, *J. Organomet. Chem.* **1993**, *450*, 209; b) M. I. Bruce, B. D. Kelly, B. W. Skelton, A. H. White, *J. Organomet. Chem.* **2000**, *604*, 150; c) M. I. Bruce, L. I. Denisovich, P. J. Low, S. M. Peregudova, N. A. Ustynyuk, *Mendeleev Commun.* **1996**, 200; d) M. I. Bruce, P. J. Low, K. Costuas, J.-F. Halet, S. P. Best, G. A. Health, *J. Am. Chem. Soc.* **2000**, *122*, 1949.
[14] a) S. N. Miligan, R. D. Rieke, *Organometallics* **1983**, *2*, 171–173; b) R. D. Rieke, S. N. Miligan, L. D. Schulte, *Organometallics* **1987**, *6*, 699.
[15] a) N. G. Connelly, A. R. Lucy, J. D. Payne, A. M. R. Galas, W. E. Geiger, *J. Chem. Soc. Dalton Trans.* **1983**, 1879; b) M. J. Freeman, A. G. Orpen, N. G. Connelly, I. Manners, S. J. Raven, *J. Chem. Soc. Dalton Trans* **1985**, 2283.
[16] a) J. Edwin, W. E. Geiger, *J. Am. Chem. Soc.* **1990**, *112*, 7104; b) W. E. Geiger, A. Salzer, J. Edwin, W. von Philipsborn, U. Piantini, A. L. Rheingold, *J. Am. Chem. Soc.* **1990**, *112*, 7121.
[17] a) M. Lacoste, F. Varret, L. Toupet, D. Astruc, *J. Am. Chem. Soc.* **1987**, *109*, 6504; b) D. Astruc, M. Lacoste, L. Toupet, *J. Chem. Soc. Chem. Commun.* **1990**, 558; c) M. Lacoste, H. Rabaa, D. Astruc, N. Ardoin, F. Varret, J.-Y. Saillard, A. LeBeuze, *J. Am. Chem. Soc.* **1990**, *112*, 9548; d) M.-H. Delville, M. Lacoste, D. Astruc, *J. Am. Chem. Soc.* **1992**, *114*, 8310.
[18] M. Watanabe, M. Sato, *Organometallics* **1999**, *18*, 5201.
[19] a) M. Sato, Y. Kawata, A. Kudo, A. Iwai, H. Saitoh, S. Ochiai, *J. Chem. Soc. Dalton Trans.* **1998**, 2215; b) M. Sato, A. Kudo, Y. Kawata H. Saitoh, *Chem. Commun.* **1996**, 25.
[20] M. Sato, M. Watanabe, *Chem. Commun.* **2002**, 1574.
[21] C.-F. Chiu, M. Song, B.-H. Chen, K. S. Kwan, *Inorg. Chim. Acta* **1997**, *266*, 73–79.
[22] a) T. Kuwata, D. E. Bublitz, G. Hoh, *J. Am. Chem. Soc.* **1960**, *82*, 5811; b) D. E. Bublitz, T. Kuwata, G. Hoh, *Chem. Ind.* **1959**, *78*, 356.
[23] S. Barlow, A. Cowley, J. C. Green, T. J. Brunker, T. Hascall, *Organometallics* **2001**, *20*, 5351.
[24] W. E. Geiger, *Prog. Inorg. Chem.* **1985**, *33*, 275.
[25] D. O. Cowan, G. A. Candela, and F. Kaufman, *J. Am. Chem. Soc.* **1971**, *93*, 3889.
[26] W. H. Morrison, S. Krogsrud, D. N. Hendrickson, *Inorg. Chem.* **1973**, *12*, 1998.
[27] The attempt of the quantitative correlation between the redox potential and the HOMO energy is reported in the binuclear complexes. F. Fabrizi de Biani, M. Fontani, E. Ruiz, P. Zanello, J. M. Russell, R. N. Grimes, *Organometallics* **2002**, *21*, 4129.
[28] K. Unoura, A. Iwase, H. Ogino, *J. Electroanal. Chem. Interfacial Electrochem.* **1990**, *295*, 385.
[29] G. Balacco, *J. Chem. Inf. Comput. Sci.* **1994**, *34*, 1235.
[30] A. R. Kudinov, M. I. Rybinskaya, Yu. T. Struchkov, A. I. Yanovskii, P. V. Petrovskii, *J. Organomet. Chem.* **1987**, *336*, 187.
[31] S. Kamiyama, T. M. Suzuki, T. Kimura, A. Kasahara, *Bull. Chem. Soc. Jpn.* **1978**, *51*, 909.
[32] U. T. Mueller-Westerhoff, Z. Yang, G. Ingram, *J. Organomet. Chem.* **1993**, *463*, 163.
[33] Gaussian 98 (Revision A.7), M. J. Frisch, G. W. Trucks, H. B. Schlegel, G. E. Scuseria, M. A. Robb, J. R. Cheeseman, V. G. Zakrzewski, J. A. Montgomery, Jr., R. E. Stratmann, J. C. Burant, S. Dapprich, J. M. Millam, A. D. Daniels, K. N. Kudin, M. C. Strain, O. Farkas, J. Tomasi, V. Barone, M. Cossi, R. Cammi, B. Mennucci, C. Pomelli, C. Adamo, S. Clifford, J. Ochterski, G. A. Petersson, P. Y. Ayala, Q. Cui, K. Morokuma, D. K. Malick, A. D. Rabuck, K. Raghavachari, J. B. Foresman, J. Cioslowski, J. V. Ortiz, B. B. Stefanov, G. Liu, A. Liashenko, P. Piskorz, I. Komaromi, R. Gomperts, R. L. Martin, D. J. Fox, T. Keith, M. A. Al-Laham, C. Y. Peng, A. Nanayakkara, C. Gonzalez, M. Challacombe, P. M. W. Gill, B. G. Johnson, W. Chen, M. W. Wong, J. L. Andres, M. Head-Gordon, E. S. Replogle, J. A. Pople, Gaussian, Inc., Pittsburgh, PA, **1998**.
[34] A. D. Becke, *J. Chem. Phys.* **1993**, *98*, 5648.
[35] C. Lee, W. Yang, R. G. Parr, *Phys. Rev. B* **1988**, *37*, 785.
[36] GaussViewW, Version 2.1 Gaussian Inc., **2000**.

Received: December 9, 2003 [F6004]